國立台灣大學醫學院生物化學暨分子生物學研究所

博士論文

Graduate Institute of Biochemistry and Molecular Biology

College of Medicine

National Taiwan University

Doctoral Dissertation

CRN-5 與 Rrp46 參與核酸降解的結構及功能性研究

Structural and Functional Studies of CRN-5 and Rrp46 in Apoptotic DNA Degradation

楊哲權

Yang, Che-Chuan

指導教授：袁小玲　博士

Advisor: Hanna S. Yuan, Ph. D.

中華民國九十九年七月

July, 2010

CONTENTS

CONTENT OF TABLES

CONTENT OF FIGURES

中文摘要

Rrp46 原本是真核生物外切體(exosme)的組成蛋白之一；外切體複合物(exosome complex) 是一參與核醣核酸分解的重要的核醣核酸外切酶(exoribonuclease)，可從單股的核醣核酸之 3'端往 5'端逐一進行分解作用，同時調控細胞內各種核醣核酸的生成與降解，此功能維繫了細胞活性的正常。因此，Rrp46 也是組成外切體複合物及維持細胞正常生長所必需。

在蛋白質分類上，Rrp46 屬於 RNase PH 外切酶家族。此類核醣核酸分解酵素(RNase)，廣泛保留在從原核生物(prokaryotes)到真核生物(eukaryotes)的各類生物體中，包括細菌、古代菌(archaea)、酵母菌，乃至於植物與人類。在線蟲(*C. elegans*)當中，CRN-5 是 Rrp46 的同源蛋白質(homologue)；被發現可能另外當作細胞凋亡(apoptosis)時，參與分解染色體去氧核醣核酸(chromosomal DNA)的新功能。本篇論文即結合了生化分析、生物物理及蛋白質晶體結構等方法，來探討 Rrp46 及 CRN-5 降解 DNA 及 RNA 時的生化特性及生理功能，為此類 RNase PH 外切酶的新功能提出更有利的佐証。

在此篇論文中，我們提出了 CRN-5 以及稻米 Rrp46 (oRrp46)的蛋白質晶體結構，它們的最高解析度分別是 3.9 Å 及 2.0 Å。經由分析三個不同物種(人類、稻米及線蟲)的 Rrp46 重組蛋白質發現，它們以二具體(homodimer)的形式存在於體外。除了已知與外切體複合物結合外，我們也首次觀察到此二具體形式的 Rrp46 亦同時存在人類與稻米細胞環境中。由生化生析的結果，發現稻米二具體 oRrp46 重組蛋白質除了具有磷酸分解(phosphorolysis)RNA 的活性外，更首次發現能水解(hydrolysis)DNA 的生化活性；人類的 hRrp46 及線蟲的 CRN-5 蛋白則只具有結合 DNA，而不具分解 DNA 的活性。藉由蛋白質晶體結構與突變技術，我們分析稻米 oRrp46 活性區域以及受質結合區裡的重要胺基酸殘基所扮演的角色。發現 E160Q 的突變會明顯抑制稻米 oRrp46 的 DNA 水解活性，對分解 RNA 的影響則有限；但是 K75E/Q76E 的突變，則同時抑制了稻米 oRrp46 對 DNA 及 RNA 的結合與分解。CRN-5 本身雖沒有 DNA 分解活性，但經實驗確認，它能與另一個

細胞凋亡核酸水解酶 (apoptotic nuclease) CRN-4 有直接的結合作用，並且增強 CRN-4 的 DNA 水解活性。推測了這兩個蛋白質可能在細胞凋亡時分解 DNA 有協同作用。

綜合以上強力的研究證據，我們推測 Rrp46 蛋白質會穩定形成外切體複合物以外的二具體；此二具體可能依照不同的物種，或直接扮演有活性的組成份，或扮演結構性組成份，參與細胞凋亡時分解 DNA 的重要生理機制。

關鍵詞:核醣核酸之轉化，去氧核醣核酸之降解，晶體結構，去氧核醣核酸分解酵素 PH，核醣核酸分解酵素，去氧核醣核酸分解酵素，細胞凋亡核酸水解酵素。

ABSTRACT

Rrp46 was first identified as a protein component of the eukaryotic exosome, a protein complex involved in 3' processing of RNA during RNA turnover and surveillance. The *C. elegans* Rrp46 homologue, CRN-5, was subsequently characterized as a cell death-related nuclease, participating in DNA fragmentation during apoptosis. Rrp46/CRN-5 has a conserved RNase PH domain, usually identified in 3'-to-5' exoribonucleases. To determine how an RNase PH protein could bind and digest DNA during apoptosis, we combined biochemical, biophysical and crystal structural approaches to study Rrp46/CRN-5 from various species, including human, rice and *C. elegans*.

We have determined the crystal structures of CRN-5 and rice Rrp46 (oRrp46) at a resolution of 3.9 Å and 2.0 Å, respectively. We found that recombinant human Rrp46 (hRrp46), oRrp46, and CRN-5 are homodimers, and that endogenous hRrp46 and oRrp46 also form homodimers in a cellular environment, in addition to their association with a protein complex. Dimeric oRrp46 had both phosphorolytic RNase and hydrolytic DNase activities, whereas hRrp46 and CRN-5 bound to DNA without detectable nuclease activity. Site-directed mutagenesis in oRrp46 abolished either its DNase (E160Q) or RNase (K75E/Q76E) activities, confirming the critical importance of these residues in catalysis or substrate binding. Moreover, CRN-5 directly interacted with the apoptotic nuclease CRN-4, and enhanced the DNase activity of CRN-4, suggesting that CRN-5 cooperates with CRN-4 in apoptotic DNA degradation. Taken together all these results strongly suggest that Rrp46 forms a homodimer separately from exosome complexes and, depending on species, is either a structural or catalytic component of the machinery that cleaves DNA during apoptosis.

Keywords: RNA turnover, DNA degradation, Crystal Structure, RNase PH, RNase, DNase, apoptotic nuclease.

1. INTRODUCTION

RNA turnover and DNA degradation are traditional viewed as two independent cellular events, regulated and executed by different sets of proteins. In this thesis we provide lines of evidence to show that a protein, named Rrp46, participates and links between the two events of RNA and DNA degradation. The overview of the two groups of proteins involved in apoptotic DNA fragmentation and RNA turnover are described below in this chapter.

1.1 Apoptotic DNA fragmentation by nucleases

Apoptosis, or programmed cell death, is an evolutionary conserved and highly regulated process that is essential for development, homeostasis and self-defense against virus infection. Improper regulation of apoptosis can lead to diseases including cellular transformation, degenerative disorders and autoimmune diseases.

One of the hallmarks of apoptosis is the fragmentation of chrosomal DNA, a point of no return to eliminate the ability of a cell to replicate its genome and to transcribe its genes. The chrosomal DNA in apoptotic cell is condensed and then degraded into fragments of multiplies of ~180-bp DNA ladders (Figure 1-1) (Wyllie, 1980). The ladder is a consequence of the cleavage of chromatin by endonucleases that target the linker DNA between the nucleosomes. Further digestion of these long DNA ladders into nucleotides recycles these biomolecular materials for healthy cells. Multiple of deoxyribonucleases (DNase) have been implicated in executing apoptotic DNA fragmentation and degradation, including 40-kD DNA fragmentation factor (DFF40, also known as caspase activated DNase (CAD)), Endobuclease G (EndoG), and deoxyribonuclease II (DNase II)(Parrish and Xue, 2006; Samejima and Earnshaw, 2005).

1.2 DFF40/CAD and Dicer are caspase-activated DNases in mammals and C. elegans, respectively

Human DFF40/CAD is the best-characterized apoptotic nuclease and functions exclusively during apoptosis (Enari et al., 1998; Halenbeck et al., 1998; Liu et al., 1998; Liu et al., 1997). It functions as an endonuclease in excuting the first cut of chrosomal DNA during apoptosis. DFF40/CAD and its inhibitory chaperone DFF45 (also known as ICAD : inhibitor of CAD) form a stoichiometric 1:1 inactive complex in living cells (Figure 1-2). Following induction of apoptosis, caspase 3, caspase 7 and/or granzyme B cleave DFF45/ICAD to release and activate DFF40/CAD (Liu et al., 1997; Sakahira et al., 1998; Thomas et al., 2000; Wolf et al., 1999). DFF40/CAD then associates with chromosomal proteins such as histone H1, HMG (high mobility group) proteins, and topoisomerase II to promote cleavage of internucleosomal DNA and generate 3′ hydroxyl DNA breaks that can be detected by the TUNEL (Terminal deoxynucleotidyl transferase-mediated dUTP nick end labeling) assay (Figure 1-1) (Durrieu et al., 2000; Liu et al., 2003b; Liu et al., 1999; Toh et al., 1998). The chromosomal DNA are digested into 50- to 300-kb cleavage products and subsequently to internucleosomal DNA fragments (Widlak et al., 2000). Further degradation of chromosomal DNA fragments is likely achieved by other apoptotic nucleases that resolve the TUNEL-reactive DNA breaks or by DNase II from phagocytes once apoptotic cells are engulfed. In mice deficient in DFF40/CAD or DFF45/ICAD, and mice expressing a caspase-resistant DFF45/ICAD mutant, cells show severe defects in chromatin condensation and fragmentation during apoptosis, demonstrating that DFF40/CAD activity is required for apoptotic DNA degradation. (Kawane et al., 2003; McIlroy et al., 1999; Zhang et al., 1998).

DFF40/CAD and DFF45/ICAD homologues have been identified in human, mouse and fly (Mukae et al., 2002; Yokoyama et al., 2000). However, no DFF40/CAD and

DFF/45 homologue has been identified in *C. elegans* or in yeast where cell death and nuclear DNA degradation also occur. It was recently discovered that the parallel player of DFF40/CAD in *C. elegans* is Dicer (DCR-1) (Nakagawa et al., 2010), an RNase important for gene silencing in RNAi. In RNAi, it processes precursor dsRNA into small duplex RNA species of ~ 21 to 25 nucleotides that then incorporated into RNA-induced silencing complex (RISC) (Duchaine et al., 2006; Elbashir et al., 2001; Hutvagner et al., 2001; Lee et al., 2004; Liu et al., 2004; Liu et al., 2003a; Pham et al., 2004; Rivas et al., 2005; Zhang et al., 2002; Zhang et al., 2004). As an apoptotic nuclease, DCR-1 is cleaved by CED-3 caspase to generate a C-terminal fragment with DNase activity, which produces 3′ hydroxyl DNA breaks on chromosomes and promotes apoptosis (Nakagawa et al., 2010). The DNase activity independent from RNase activity of DCR-1 illustrates the conservation of caspase-mediated activation of apoptotic DNA fragmentation among various species.

1.3 Endonuclease G is a mitochondrial apoptotic nuclease

DFF40-deficient mammalian cells display residual apoptotic DNA fragmentation. Thus, other nucleases must be involved in cleaving chromosomal DNA during apoptosis in yeast, *C. elegans*, and mammals. Human Endonuclease G (Endo G) is another evolutionarily conserved apoptotic endonuclease that localizes to the mitochondrial intermembrane space and mediates residual apoptotic DNA fragmentation observed in DFF45/ICAD deficient cells (Li et al., 2001). Endo G together with apoptosis-inducing factor (AIF) translocate from mitochondria into nucleus during apoptosis to facilitate chromosome fragmentation (Li et al., 2001; Wang et al., 2002). The homologues of human Endo G have been found in yeast and *C. elegans* (Buttner et al., 2007; Parrish et al., 2001).It is called CPS-6 (CED-3 protease suppressor) in *C. elegans*. In a cell-free system with isolated HeLa cell nuclei, both

recombinant Endo G and CPS-6 proteins can induce generation of characteristic apoptotic DNA ladders. (Li et al., 2001; Parrish et al., 2001). In *C. elegans* deficient in *cps-6*, TUNEL-stained nuclei accumulate in mutant embryos and developmental cell death is delayed or even inhibited in sensitized genetic backgrounds (Parrish et al., 2001). These *in vitro* and *in vivo* data suggest that CPS-6 can serve as an apoptotic nuclease and is important for apoptotic DNA degradation and progression of apoptosis. The role of Endo G in mammalian apoptosis merits further study, because Endo G knockout mice show no embryonic lethality or obvious apoptotic defects (Irvine et al., 2005).

1.4 DNase II digestes apoptotic DNA fragments into nucleotides after phagocyte engulfment

The apoptotic cell divided into several apoptotic bodies contaning fragmented DNA at the late stage of apoptosis. The apoptotic bodies then were engulfed by phagocytes to complete the clearance cell debris. It is now revealed that DNase II, an acidic lysosomal DNase, in macrophage contributes the degradation of DNA from apoptotic cells (Kawane et al., 2003; McIlroy et al., 2000). In DNase II-deficient mice, although die at birth, the engulfed but not digested apoptosis cells result in large DNA-containing bodies (Kawane et al., 2003; Krieser et al., 2002). Similar results were also observed in *C. elegans* by mutating its DNase II homologue, NUC-1 (Hedgecock et al., 1983; Wu et al., 2000b). The chrosomal DNA from apoptotic cell in *nuc-1* mutants can be stained by TUNEL assays, implying that the persistant DNA are intermediates of apoptotic DNA degradation.

1.5 Cell death-related nucleases in C. elegans are also involved in apoptotic DNA degradation including CRN-5, a homologue of human hRrp46

In addition to CPS-6 and NUC-1, seven other nucleases were found to be involved in apoptotic DNA degradation in *C. elegans* by candidate-based RNAi screening (Parrish and Xue, 2003b). They are CRN-1 to -6, WHA-1 and CYP-13. CRN (cell death-related nuclease) nucleases are homologous to various human proteins with known biological functions besides apoptosis (Table 2). For example, CRN-1 is a homologue of human flap endonuclease-1(FEN-1) that is normally involved in DNA replication and repair (Harrington and Lieber, 1994; Lieber, 1997). During apoptosis in *C. elegans*, CRN-1 can associate and cooperate with CPS-6 in nuclei to promote DNA fragmentation, by using the endonuclease activity of CPS-6 and both the 5'-3' exonuclease activity and gap-dependent endonuclease activity of CRN-1(Parrish et al., 2003). CRN-4 is a member of DEDDh nuclease superfamily and is also a homologue to human 3'hExo nuclease that is normally involved in histone mRNA degradation (Dominski et al., 2003; Yang et al., 2006). In combination with crystal structural and cell death analysis in *C. elegans*, both the nuclease active site and the DNA-binding domain are required for *crn-4*'s function in apoptosis (Hsiao et al., 2009). CRN-3 and CRN-5 are homologues to exosomal components, Rrp6 and Rrp46, respectively (Liu et al., 2006). RNAi mediated depletion of *crn-5* gene results in similar cell death defects to that of *cps-6*, including accumulation of TUNEL-stained nuclei in RNAi treated embryos and inhibition of apoptosis in sensitized genetic backgrounds (Figure 1-3), indicating the involvement of CRN-5 in apoptotic DNA degradation during development of *C. elegans* (Parrish and Xue, 2003b). Moreover, CRN-5 interacts and forms another complex, called degradeosome, with CPS-6, WHA-1, CYP-13 and a number of CRN nucleases, including CRN-1 and CRN-4 (Figure 1-4) (Parrish and Xue, 2003b). Loss of any one or a combination of these *C. elegans* apoptotic nucleases

results in accumulation of TUNEL-stained nuclei, indicating this complex may function in turning the 3'-OH DNA nicks created by DCR-1 into small gaps through their exoribonuclease activities and then create double-stranded DNA breaks via a gap-dependent endonuclease activity (Parrish and Xue, 2003b; Parrish et al., 2003). These results imply that CRN-5 may be a DNase associated with the degradeosome when it is involved in DNA degradation during apoptosis.

1.6 CRN-5 is an RNase PH protein homolougous to human hRrp46 protein

Many types of RNA play a crucial role in various cellular processes, particularly as an intermediate in the translation of the genetic code into functional proteins, or as a member in post-transcriptional gene silencing. Cellular RNA molecules transcribed from DNA that undergo meticulous processing, quality control and turnover are critical in the precise expression of genetic information and even cell survival. Almost all RNA species undergo several posttranscriptional processing reactions to produce functional RNA molecules. The process is carried out by combining action of endoribonucleases (endoRNases) and exoribonucleases (exoRNases). A class of conserved exoRNase family called RNase PH (phosphorolysis) proteins is a key component involved in these processes (Symmons et al., 2002).

According to domain analysis and sequence alignment, CRN-5 protein contains an RNase PH domain and shows the highest similarity to human hRrp46 (31% idendity, Figure 1-5), an RNase PH containing component of exosome complex. Most of the RNase PH family proteins have 3' to 5' exoribonuclease activity, capable of removing the 3'-end nucleotide by adding a phosphate, rather than a water molecule, to the cleaved phosphodiester bond, and are therefore involved in phosphorolytic RNA processing and degradation ($RNA_n+Pi \rightarrow RNA_{n-1}+NDP$). Products of 'phosphorolysis' are nucleoside diphosphates rather than nucleoside monophosphates made by hydrolysis.

The first and simplest RNase PH protein discovered is RNase PH in *E. coli* with a primary role in tRNA 3' end maturation (Deutscher et al., 1988; Kelly et al., 1992; Li and Deutscher, 1994). Other examples include polynucleotide phosphorylase (PNPase) (Baginsky et al., 2001; Piwowarski et al., 2003; U.Z. Littauer and M. Grunberg-Manago, 1999) and exosome complex components (Evguenieva-Hackenberg et al., 2003; Mitchell et al., 1997).

1.7 Rrp46 is a component of exosome complex involved in RNA processing, quality control and turnover

Rrp46 (rRNA-processing 46) is an RNase PH family protein without phosphorolytic RNase activity, and was first identified as a structural component protein of the eukaryotic exosome. The exosome complex was initially identified in *Saccharomyces cerevisiae* (Allmang et al., 1999b; Mitchell et al., 1997). This complex degrades many types of RNA that have been targeted by surveillance activities in both the nucleus and cytoplasm, and it is also responsible for the precise trimming, in a 3′→5′ direction, of the 3′ ends of nuclear precursors to several RNA species.(Allmang et al., 1999a; Anderson and Parker, 1998; de la Cruz et al., 1998; Hilleren et al., 2001; Kadaba et al., 2004; Mitchell and Tollervey, 2003; Raijmakers et al., 2004; Suzuki et al., 2001; Torchet et al., 2002; van Hoof et al., 2000a). The yeast exosome core consists of ten subunit proteins with six RNase PH family proteins (Rrp41p, Rrp42p, Rrp43p, Rrp45p, Rrp46p and Mtr3p), three KH (protein K homology) and/or S1 (ribosomal protein S1 homology) RNA-binding proteins (Rrp4p, Rrp40p, and Csl4p), and an RNase II homologue (Rrp44p/Dis3p). This complex is found in both the cytoplasm and nucleus. The nuclear isoform contains an additional component, the RNase D homologue Rrp6p (Table 1) (Allmang et al., 1999b; Mitchell et al., 1997; Schmid and Jensen, 2008).

The human counterpart was identified soon after characterization of the yeast exosome. Its components turned out to be part of the previously described polymyositis/scleroderma (PM/Scl) autoantigenic multiprotein complex (Allmang et al., 1999b; Brouwer et al., 2001). Specific autoantibodies in sera of patients suffering from the autoimmune disease PM/Scl showed reactivity with this PM/Scl antigen (Reichlin et al., 1984; Treadwell et al., 1984). After the identification and cloning of two main autoantigenic proteins, PM/Scl-100 and PM/Scl-75 (Alderuccio et al., 1991; Bluthner and Bautz, 1992; Ge et al., 1992), both proteins were shown to be homologous to yeast Rrp6p and Rrp45p, respectively (Allmang et al., 1999b; Briggs et al., 1998). The human exosome core also contains six RNase-PH family proteins (hRrp41, hRrp42, hRrp43, hRrp45, hRrp46, and hMtr3) along with three KH/or S1-containing subunits (hRrp4, hRrp40, and hCsl4) (Tabel 1). Related Rrp46s and exosomes have been described in other species, such as among the hyperthermophilic archaea, nematodes, unicellular parasites, flies, and plants (Allmang et al., 1999b; Andrulis et al., 2002; Chekanova et al., 2000; Estevez et al., 2001; Evguenieva-Hackenberg et al., 2003; Koonin et al., 2001; Liu et al., 2006). Although most cells have other enzymes that can degrade and process RNA, each core subunit of the exosome, including Rrp46, is essential for cell survival (Allmang et al., 1999b; van Dijk et al., 2007). This reveals the indispensable and irreplaceable function of exosome complex in various species.

In nucleus, the exosome functions in the 3′ processing of the precursors to stable RNAs, including the 5.8S rRNA component of mature ribosomes, snRNAs and snoRNAs (Allmang et al., 1999a; de la Cruz et al., 1998; van Hoof et al., 2000a; Zanchin and Goldfarb, 1999). It is also responsible for the surveillance and degradation of aberrant nuclear precursors of many types of RNA including pre-mRNAs, pre-tRNAs, pre-rRNAs (Allmang et al., 2000; Bousquet-Antonelli et al., 2000; Burkard and Butler, 2000; Kadaba et al., 2004; Torchet et al., 2002) and other highly unstable non-coding

transcripts, termed cryptic unstable transcripts (CUTs) (Figure 1-6)(Arigo et al., 2006b; Thiebaut et al., 2006).

In cytoplasm, the only known substrates for exosome are mRNAs (Figure 1-6). The exosome participates in the 3′ turnover of normal mRNA to regulate the level of mRNA and the rate of protein synthesis (Anderson and Parker, 1998; van Hoof et al., 2000a). Also, the exosome rapidly degrades aberrant mRNAs with structural defects in NMD (nonsense-mediated decay) pathway (Lejeune et al., 2003; Mitchell and Tollervey, 2003; Takahashi et al., 2003). In human cells, the exosome is also recruited to, and rapidly degrades, short-life spanned mRNAs that contain specific AU-rich sequence elements (AREs) (Chen et al., 2001; Gherzi et al., 2004; Mukherjee et al., 2002; Tran et al., 2004). Furthermore, the exosome degrades the 5′ fragments of mRNAs that are cleaved in the NGD (no-go decay) pathway, which targets mRNAs on which translation has stalled (Doma and Parker, 2006). It also plays a role in antiviral defence by degrading viral mRNA (Guo et al., 2007). The 5′ fragments of mRNAs that have been cleaved by the RNA interference (RNAi) pathway in *Drosophila melanogaster* cells are similarly degraded by the exosome (Orban and Izaurralde, 2005).

1.8 The structures of RNase PH proteins and exosome complex

The six RNase PH family proteins in the human exosome form a ring-like hexamer structure as revealed by the crystal structure analysis of the exosome core (Figure 1-7) (Liu et al., 2006). The ring consists of three distinct heterodimers built from six different proteins, hRrp41-hRrp45, hRrp46-hRrp43 and hMtr3-hRrp42 and each hRrp protein shares typical β-α-β-α RNase PH folding. Additional subunits (hRrp4, hRrp40, and hCsl4) play as a cap to stabilize the core exosome. A similar hexameric-ring structural organization is conserved in other RNase PH family proteins including bacterial RNase PH (Harlow et al., 2004b; Ishii et al., 2003b), PNPase (Shi et al., 2008;

Symmons et al., 2000) and archaeal exosome core complex (Buttner et al., 2005; Lorentzen and Conti, 2005; Lorentzen et al., 2005; Navarro et al., 2008) (Figure 1-7). The archaeal exosome is a simplified version of the eukaryotic complex. The two archaeal RNase PH family proteins, aRrp41 and aRrp42, form a hexameric ring composed of three copies of stable catalytically active aRrp41-aRrp42 heterodimers. The phosphorolytic exonuclease active sites of the archaeal exosome are situated in the internal 'processing chamber' of the aRrp41-aRrp42 ring. Only aRrp41 has an RNase active site, whereas aRrp42 is required for complex assembly and activity (Buttner et al., 2005; Lorentzen and Conti, 2005; Lorentzen et al., 2005; Navarro et al., 2008). One or both of the S1 and KH domain-containing RNA-binding proteins, aRrp4 and aCsl4, are positioned on top of the basal ring. They are important for substrate binding and recognition (Stickney et al., 2005). The constricted entrance to the central channel is only 8–10 Å wide, which allows only single-stranded RNA to enter the catalytic cavity (Lorentzen et al., 2007; Navarro et al., 2008). This may explain why isolated archaeal exosomes degrade only substrates containing single-stranded 3' ends.

1.9 Recombinant human and yeast exosomes are inactive in phosphorolysis

E. coli RNase PH itself forms a homo-hexameric ring similar to the exosome (Figure 1-7) (Harlow et al., 2004b; Ishii et al., 2003b). PNPase is a homotrimer of subunits that each contains two RNase PH-type domains (Figure 1-7) (RNase PH_I and RNase PH_II), organized in an inverted arrangement similar to the individual subunits of RNase PH. In addition, each PNPase monomer contains two RNA-binding domains in the C-terminus: one S1 type and one KH type, which are similar to those found in the eukaryotic exosome cap proteins (Leszczyniecka et al., 2002; U.Z. Littauer and M. Grunberg-Manago, 1999). The PNPase forms a similar hexameric ring structure (Shi et

al., 2008; Symmons et al., 2000). Hence, all known structures of RNase PH containing proteins tend to form a stable hexameric ring among different species. The bacterial homo-hexameric RNase PH has six phosphorolytic active sites on each subunit of the ring, whereas in PNPase and archaeal exosome, this is reduced to three active sites per complex (Figure 1-7A). The active sites are located in the interface of RNase PH_I-RNase PH_II and aRrp41-aRrp42 heterodimers, whereas the active subunits are RNase PH_II and aRrp41, respectively. It is originally believed that eukaryotic exosomes show similar active RNase PH domain arrangement and carry an active site in Rrp41. However, it turns out that the recombinant yeast and human exosome cores are inactive and lack any detectable phosphorolytic exoribonuclease activity, suggesting that all of the RNase PH proteins in the ring, including hRrp46, are inactive (Dziembowski et al., 2007; Liu et al., 2006). Only when associated with Rrp44p/Dis3p (an RNase II family protein), the yeast exosome shows hydrolytic activity, but not phosphorolytic activity, which is contributed from Rrp44p/Dis3p (Dziembowski et al., 2007; Schaeffer et al., 2009). It is suggested that the yeast exosome functions as a macromolecular cage to channel RNA substrate to Rrp44p/Dis3p for degradation (Bonneau et al., 2009). This result was quite an impact on our understanding of this "dead" core exosome in eukaryotes. However, this suggestion is likely not universally true, since the exosome core in the plant lineage was suggested to have phosphorolytic activity (Chekanova et al., 2000), indicating that eukaryotic exosomes may have evolved divergent means of RNA degradation.

1.10 Cofactors regulate and activate exosome's activity

Human and yeast exosome core displays no detectable enzymatic activity in isolation. Furthermore, the variety of cellular processes, in which the exosome is

involved, raises the question how the complex is recruited to a certain substrate and guided to perform a specific function. Hence, some co-factors and complex have been identified that can regulate and activate the exosome for full activity on defined classes of transcript (Figure 1-8).

The TRAMP complex is a major co-factor for yeast nuclear exosome, which contains one of two poly(A) polymerases, Trf4 or Trf5, one of two RNA-binding proteins, Air1 or Air2, and the RNA helicase Mtr4 (Houseley and Tollervey, 2006; LaCava et al., 2005; Vanacova et al., 2005; Wyers et al., 2005). TRAMP interacts directly with the exosome and appears to function by adding unstructured oligo(A) tails to the 3' ends of exosome substrates, such tails might recruit the exosome and/or initiate degradation from 3' ends. The exosome and TRAMP complex are also recruited during transcription of RNA polymerase II transcripts such as snRNA, snoRNA and CUTs via the transcription termination factor complex Nrd1-Nab3. The Nrd1-Nab3 complex which contains minimally the RNA-binding proteins Nrd1 and Nab3, and the helicase Sen1, is implicated in promoting RNA degradation by the exosome both *in vivo* and *in vitro* (Arigo et al., 2006a; Thiebaut et al., 2006; Vasiljeva and Buratowski, 2006).

Cytoplasmic activity of yeast exosome requires another set of co-factor: Ski7, a GTPase with homology to translation factor EF1α, and the SKI complex composed of Ski2, Ski3 and Ski8 (Araki et al., 2001; Brown et al., 2000; Inada and Aiba, 2005; van Hoof et al., 2000b; Wang et al., 2005). Ski7 interacts both with the SKI complex and the exosome, and is a general co-factor in these processes. Ski2 is an RNA helicase that is homologous to Mtr4. The SKI complex is involved in the NMD and NGD mRNA surveillance pathways (Inada and Aiba, 2005; Mitchell and Tollervey, 2003; Takahashi et al., 2003; van Hoof et al., 2002).

How these co-factors actually activate and promote the RNase activity of exosome is still under investigation, but they indeed provide a platform for physical recruitment

of the exosome to specific RNA substrates, which plays a key role in stimulating RNA degradation in both the nucleus and the cytoplasm.

1.11 hRrp46 is a broadly immunogenic antigen, which is overexpressed in tumor cells

hRrp46 is also named CML28, as it is a 28 kD antigen abundant in the sera of chronic myelogenous leukemia (CML) patients after allogeneic hematopoietic stem cell transplantation (Wu et al., 2000a). In patients with CML who have relapsed after bone marrow transplantation (BMT), infusion of donor lymphocytes induces durable remission in 70–80% of patients (Collins et al., 1997; Kolb et al., 1990; Kolb et al., 1995). In order to identify the target antigens of this immune response, a CML cDNA expression library has been screened from CML post-DLI responder sera (Wu et al., 2000a). One of the antigens identified as a potential tumor-associated target in DLI responders is termed CML28, a 28-kD protein identical to hRrp46 (Yang et al., 2002).

Additional analysis shows that hRrp46/CML28 mRNA is highly expressed in different tumors than in normal tissues. The protein level is also high in highly proliferative tumors such as AML (acute myelogenous leukemia) and blast crisis CML. In contrast, hRrp46/CML28 protein was undetectable or present at very low levels in normal bone marrow and peripheral blood. hRrp46/CML28 has therefore been further evaluated as an immunotherapy target for the stimulation of anti-tumor immune response (Xie et al., 2008; Zhou et al., 2006).These observations demonstrate that hRrp46/CML28 antigen is immunogenic in patients with a variety of different solid tumors.

1.12 Auto-antibodies against hRrp46 are also found in patients with autoimmune diseases

The development of high titer antibody against hRrp46/CML28 correlated well

with the cytogenetic remission induced by DLI. IgG antibodies specific for hRrp46/CML28 were also found in 10–33% of patients with melanoma, lung, and prostate cancer (Yang et al., 2002). Intriguingly, auto-antibodies against hRrp46, and the exosome component protein PM-Scl100/Rrp6, are often found in patients with autoimmune diseases, including scleroderma, PM/Scl overlap syndrome and idiopathic inflammatory myopathy (Bluthner and Bautz, 1992; Brouwer et al., 2002; Ge et al., 1992; Reichlin et al., 1984). It is not clear why hRrp46 or antibodies against hRrp46 are highly expressed in cancers and auto-immune diseases but these results do hint, albeit vaguely, at a connection between hRrp46 expression and cell survival.

1.13 Specific aims

The RNase PH and exosome systems play essential roles in regulating functional RNA formation and degradation that are critical for cell survival. On the contrary, apoptotic nucleases degrade chrosomal DNA into nucleotides for recyling and eliminating autoimmue materials during cell death. These two systems seem not related until the discovery of RNase PH and exosomal component Rrp46/CRN-5 participating in apoptotic DNA degradation using RNAi technology (Parrish and Xue, 2003b). With an RNase PH domain, Rrp46 plays an essential structural but not catalytic role in exosome complex for RNA maturation and degradation. On the other hand, the finding of *crn-5* knockdown *C. elegans* displayed defects in apoptotic DNA degradation during development similar to that in *cps-6* knockdown model. These observations implied that Rrp46/CRN-5 could play a dual role in different stages of cell survival and death, and it links between RNA dedradation in RNA turnover and DNA fragmentation in apoptosis. We hypothesize that Rrp46/CRN-5 associates with exosome and is involved in RNA processing and degradation in living cells. During apoptosis, it switches its role to a DNase, and participates in apoptotic DNA degradation (Figure 1-9). Because the

evoluted variation in RNase PH proteins among species, we use Rrp46/CRN-5 proteins from three different species, rice, nematodes and human. We characterize the three proteins using mutational, biochemical, biophysical and structural approaches. Our specific aims are as followed:

1. To characterize if Rrp46 folds independently by itself.
2. To determine if Rrp46 has DNase and/or RNase activity.
3. To determine the substrate preference for Rrp46.
4. To characterize the structural basis for DNase and/or RNase activity of Rrp46.
5. To determine how to regulate the activity of Rrp46 in normal cells and apoptotic cells.

In this thesis, we found that Rrp46 forms stable homodimer in addition to a component in exosome complex by biophysical and structural analysis. This homodimeric Rrp46 is capable of binding to DNA. Moreover, for the first time, rice oRrp46 was demonstrated here to be able to digest DNA in a metal ion-dependent manner. Although CRN-5 shows no detectable DNase activity, it enhances another apoptotic DNase, CRN-4's, activity. These findings support the new structural or DNase role of Rrp46/CRN-5 in apoptotic DNA degradation. In combination of biochemical, mutagenesis and structural approaches, our results also show the critical importance of some residues in catalysis or substrate binding of rice oRrp46. This result suggests that RNase PH proteins have evolved into active and inactive RNases. Our findings therefore suggest that Rrp46 is a dual-function protein: when associated with exosome, it is involved in RNA processing and turnover in normal cells, and when it forms a homodimer, or associated with degradeosome complex, it is involved in DNA degradation during apoptosis. This finding therefore provides a new direction for the study of the role of hRrp46 in cancer and autoimmune diseases.

2. MATERIALS AND METHODS

2.1 Cloning, protein expression, and purification

The full-length cDNAs of human and of rice Rrp46 were purchased from OpenBiosystems (Clone ID: 4308795) and the KOME database (Clone ID: 204796), respectively. The genes of the full-length rice Rrp46 (oRrp46) (residues 1-238), CRN-5 (residues 1-215) and human Rrp46 (hRrp46) (residues 1-236) were PCR-amplified and cloned into expression vectors, pET-22b (Novagen), pQE-70 (Qiagen) and pET-28c (Novagen), respectively, to generate His-tagged fusion constructs. pQE-70-CRN5 expression plasmid was transformed into *E. coli* M15 strain cultured in LB medium, supplemented with 100 μg/mL ampicillin. pET-22b-oRrp46 and pET-28c-hRrp46 were transformed into *E. coli* BL21-CodonPlus(DE3)-RIPL strain (Stratagene) cultured with 75 μg/mL streptomycin, 50 μg/mL chloramphenicol and 100 μg/mL ampicillin or 50 μg/mL kanamycin. The transformed bacterial expression strains were grown to an OD600 of 0.4, and then induced with 0.5 mM IPTG at 18°C for 20 hours. The harvested cells were disrupted by a microfluidizer in the buffer of 50 mM Tris-HCl (pH 7.6), 300 mM NaCl and 1 mM β-mercaptoethanol.

Procedures of protein purification below were operated under 4°C. Crude cell extracts were first loaded onto a TALON metal resin affinity column (BD Biosciences). After washing with buffer A (50 mM Tris-HCl pH 7.6, 300 mM NaCl and 1 mM β-mercaptoethanol) + 3%-5% buffer B (50 mM Tris-HCl pH 7.6, 300 mM NaCl, 500 mM imidazole and 1 mM β-mercaptoethanol) (3% for rice oRrp46, 5% for CRN-5 and human hRrp46, respectively), proteins were eluted using a imidazole gradient (buffer B). The CRN-5/Rrp46-containing fractions were then concentrated to 2 ml and applied to a gel filtration chromatography column (Superdex 200, GE Healthcare) in a running

buffer of 25 mM Tris-HCl (pH 7.6), 150 mM NaCl and 1 mM β-mercaptoethanol. Purified protein samples were then concentrated to a suitable concentration and stored in a -80°C refrigerator. The homogeneity of the protein was analyzed by electrophoresis. Protein samples (2 μg) were mixed with 1x sample loading buffer (35 mM Tris-HCl, pH 7.0, 1 mM EDTA, 2% SDS, 4% sucrose, 0.002% bromophenol blue and 6 mM β-mercaptoethanol) and were heated (95°C) for 5 min to denature the protein before resolving the sample in 10% SDS-PAGE stained with commassie blue (see Figure 3-1B). All oRrp46 point mutants were generated by Quickchange site-directed mutagenesis kits (Stratagene) and purified by the same procedure as the wild-type oRrp46. The designed primers for rice oRrp46(E160Q) were 5'-GGACACAAACAAAGCAGAACAGCAGCAATTGAAATCATTTGC-3' and 5'-GCAAATGATTTCAATTGCTGCTGTTCTGCTTTGTTTGTGTCC-3'. The designed primers for rice oRrp46(K75E/Q76E) were 5'-CAGATTGGGGAGGAGGAGAAGGAGTATGAG-3' and 5'-CTCATACTCCTTCTCCTCCTCCCCAATCTG- 3'.

2.2 Dynamics light scattering (DLS) and analytical ultracentrifugation (AUC)

DLS measurements were carried out on a Dyna-Pro 99 MS800 instrument (Protein Solutions). The purified protein (0.5 mg/mL) in a buffer of 20 mM HEPES (pH 7.0), 100 mM NaCl, 1 mM $CaCl_2$ and 1 mM DTT was centrifuged at 16,000 g, 4°C for 15 min, and the supernatant was placed in a 12-μL cuvette (b = 1.5 mm). The protein samples were incubated for 5 min at 20°C before data acquisition over an acquired time of 15 min. The size distribution plots, the x axis showing a distribution of estimated particle radius (nm) and the y axis showing the relative intensity of the scattered light (% of intensity), were analyzed with the software Dynamics V5.26.60 (Protein Solutions).

For AUC assays, the recombinant human hRrp46 and *C. elegans* CRN-5 were concentrated to an OD_{280} of 0.5 in 25 mM Tris-HCl (pH 7.6), 150 mM NaCl and 1 mM β-mercaptoethanol. Sedimentation velocities of proteins were performed at 40,000 rpm (Beckman XL-A) under 4°C. Multiple scans (OD_{280}) at different time intervals were then fitted to a continuous c(s) distribution model using the SEDFIT program (Brown and Schuck, 2006; Schuck, 2000).

2.3 Fractionation of cell extracts and western blotting

$2x10^7$ human kidney 293T cells were washed with PBS buffer (10 mM Na_2HPO_4, 1.8 mM KH_2PO_4, pH 7.4, 140 mM NaCl and 2.7 mM KCl) twice and then pooled and extracted by sonication in 2 ml of cold PBS with or without 1 mM β-mercaptoethanol. Rice callus cells were dried by filter paper and extracted by grinding in liquid nitrogen, then dissolved in 2 ml PBS buffer. Crude cell extract was then centrifuged at 16,000 g, 4°C for 15 min. The supernatant was collected and passed through a gel filtration chromatography column (Superdex 200, GE Healthcare) in a running buffer of PBS. Eluted fractions were collected and concentrated using Vivaspin 6 centrifugal concentrators (GE Healthcare). Equal volumes of concentrated fractions were separated by 10% SDS-PAGE, and then transferred to immobilon-P (Millipore) PVDF membrane. Membranes were then probed by first antibody (anti-hRrp46/2,000x dilution, anti-oRrp46/5,000x dilution and anti-hRrp42/2,000x dilution antibodies, respectively). After incubated with alkaline phosphatase (AP)-conjugated secondary antibodies, the signals were developed by adding NBT/BCIP (Perkin Elmer Life Science).

2.4 DNA-binding and DNase activity assays

For DNA gel shift assays, 20 nM of 5'-end P^{32}-labeled 20-nucleotide

double-stranded DNA (5'-ACTGGACAAATACTCCGAGG-3') were incubated with different concentrations of purified recombinant protein in a buffer containing 20 mM HEPES (pH 7.0) and 5 mM EDTA on ice for 1 hr. After incubation, the reaction mixtures were resolved in 10% polyacrylamide gels, which were exposed to the phosphorimaging plate (Fujifilm) and analyzed by an FLA-5000 (Fujifilm) imaging system (Figures 3-5A and 3-15C).

For the DNase activity assays shown in Figures 3-6A, 3-6B and 3-15A, 309-bp linear double-stranded DNA (30 nM) were incubated with the purified protein (1 μM) in the DNase reaction buffer containing 20 mM HEPES (pH 7.0), 100 mM NaCl, 1 mM $CaCl_2$ and 1 mM DTT, at 37°C for the indicated periods. For the DNase activity assays shown in Figure 3-6C, a pQE-70 plasmid DNA (100 ng) was incubated with 0.2 μM purified protein in the DNase reaction buffer at 37°C for the indicated periods. Identical substrate was used in Figure 3-10B. For the DNase activity assays shown in Figure 3-16, purified CRN-4 and/or CRN-5 (concentration 1-2 μM) was incubated with 309-bp double-stranded DNA (30 nM) in a solution of 10 mM NaCl, 3 mM $MgCl_2$, 1 mM $CaCl_2$ and 20 mM Tris-HCl (pH 6.0) at 30°C for 40 minutes. All the reactions were stopped by adding 10 mM proteinase K for 10 min to remove proteins. The digest patterns were resolved on 1% or 1.5% agarose gels stained by ethidium bromide, and quantified by AlphaEaseFC software (Alpha Innotech).

2.5 RNA-binding and RNase activity assays

The 2.3 kb ssRNA was transcribed *in vitro* using a MAXIscript kit (Ambion). The 20-mer ssRNA (5'-ACUGGACAAAUACUCCGAGG-3') was first labeled at the 5' end with [γ-^{32}P] ATP by T4 polynucleotide kinase and then purified on a Microspin G-25

column (GE Healthcare) to remove the unincorporated nucleotides. For RNA binding assays, 500 ng of 2.3 kb ssRNA substrates were incubated with different concentrations of recombinant purified protein in the RNA binding buffer (50 mM Tris-HCl pH 8.0 and 10 mM EDTA) on ice for 30 min. After incubation, the reaction mixture was separated on 1% agarose gels and stained with ethidium bromide.

For RNase activity assays, 20 nM of labeled 20-mer ssRNA or 500 ng 2.3 kb ssRNA substrates were incubated with different concentrations of purified protein in the RNase reaction buffer (50 mM Tris-HCl pH 8.0, 50 mM KCl, 2 mM $MgCl_2$, 5 mM NaH_2PO_4 and RNaseIN (1 U/μl, Promega)) at 30°C for 1 hour. The reaction was stopped at the time point indicated in the figures by adding TBE-Urea sample buffer (Bio-Rad) or 10 mM proteinase K. Digest patterns of 20-mer ssRNA were resolved in 20% polyacrylamide/7 M urea gels, which were exposed to the phosphorimaging plate (Fujifilm) and analyzed by an FLA-5000 (Fujifilm) imaging system.

The RNA substrate used in the thin layer chromatography (Figure 3-7C) was transcribed by T7 RNA polymerase with linearized (*Xho*I) pET-22b (Novagen) in the presence of [α-^{32}P]ATP. Ascending thin layer chromatography was done on polyethyleneimine-cellulose plates (Sigma) in 1.2 M formic acid and 0.5 M LiCl. The cold AMP and ADP standards (100 nmol) were added to the samples before loading. Standards were visualized by UV shadowing.

2.6 Crystallization and X-ray diffraction data collection

Crystals of CRN-5 and oRrp46 were grown by the hanging-drop vapor diffusion method at room temperature. The crystallization drop was made by mixing 1 μl of protein solution and 1 μl of reservoir solution. oRrp46 (7.5 mg/ml, 50 mM Tris-HCl, pH 8.0, 150 mM NaCl) was crystallized using a reservoir solution containing 0.2 M sodium

malonate (pH 7.0) and 20% PEG3350. CRN-5 (30 mg/ml, 50 mM Tris-HCl, pH 8.0) was crystallized using a reservoir solution containing 0.1 M Tris-HCl (pH 8.0), 0.2 M NaCl and 25% PEG3350. Diffraction data of oRrp46 and CRN-5 were collected at -150°C at beamlines 13C1 and 13B1, respectively, of the NSRRC in Hsinchu, Taiwan, and were processed and scaled by HKL2000 (Otwinowski and Minor, 1997). All diffraction statistics are listed in Table 3.

2.7 Structure determination and refinement

oRrp46 crystallized in the trigonal space group $P3_1$ as twin crystals with a twin factor of 0.5. The twin operation of the Miller index was assigned as (h,-h-k,-l) using Phenix (Xtriage) (Adams et al., 2002), as well as Merohedral Crystal Twinning Server (Yeates, 1997). CRN-5 crystallized in the monoclinic space group $P2_1$ with two molecules per asymmetric unit. The structure oRrp46 and CRN-5 were solved by molecular replacement by CCP4-Molrep (Potterton et al., 2003) and BALBES (Long et al., 2008), respectively, using the crystal structure of human Rrp46 (PDB accession code: 2NN6, chain D) as the search model. The protein model was constructed using the program Coot (Emsley and Cowtan, 2004) and refined by Phenix (Adams et al., 2002). Due to the low resolution of the CRN-5 data (3217 unique reflections), the CRN-5 structure was refined in the final stage by rigid-body refinements followed by group B factor refinements (one residue per group). The stereochemical quality of the refined model was evaluated by PROCHECK (Laskowski et al., 1993). Structural coordinates and diffraction structure factors have been deposited in the RCSB Protein Data Bank with the PDB ID code of 3HKM for oRrp46 and 3KRN for CRN-5.

2.8 His-tag pull-down assays

His-tagged CRN-5 (5 μg) was incubated with CRN-4 (5 μg) in 50 mM Tris-HCl, 300 mM NaCl pH 7.5 at 4°C for 8 hours. After centrifugation, the protein sample was loaded onto Ni-NTA spin columns (Qiagen) and washed 3 times each with Wash-1 buffer and Wash-2 buffer (Wash-1 buffer: 50 mM Tris-HCl, 300 mM NaCl (pH 7.5) and 2 mM imidazole; Wash-2 buffer: 50 mM Tris-HCl, 300 mM NaCl (pH 7.5) and 5 mM imidazole). Bound proteins eluted with Elution buffer (50 mM Tris-HCl, 300 mM NaCl (pH 7.5) and 500 mM imidazole) were separated by SDS-PAGE in 10% gels. CRN-4 and His-tagged CRN-5 were probed with anti-CRN-4 and anti-His tag antibodies (Novagen) after transferring onto a PVDF membrane. Detection was carried out using alkaline phosphatase-conjugated secondary antibody (Millipore) and BCIP/NBT substrate solution.

3. RESULTS

3.1 C. elegans' CRN-5 is a homologue to human Rrp46.

The exosome components were widely studied in the species of archaea, yeast and human. Little is known about the exosome components of *C. elegans*. The discovery of CRN-5 as a homologue of human hRrp46 was initially suggested in Parrish's paper based on sequence alignment (Parrish and Xue, 2003b). To further confirm that CRN-5 is homologous to hRrp46, but not other RNase PH proteins, we surveyed the database (WormBase, http://www.wormbase.org/) to verify 6 individual exosomal core RNase PH proteins in *C. elegans*. The result shows that each human exosomal core RNase PH protein has its own homologue in *C. elegans*, and CRN-5 has highest sequence identity (31% of identity and 48% of similarity) to hRrp46 than to others (Table 3). Liu et al. also published similar result to our study (Liu et al., 2006).

3.2 Overexpression and purification of CRN-5 and Rrp46 proteins.

Because RNase PH proteins have evolved divergently with or without nuclease activity, we decided to work on Rrp46 form three different species for enzymatic and structural analysis. The full length cDNA encoding *C. elegans* CRN-5, rice (*Oryza sativa*) oRrp46, and human hRrp46 were PCR-amplified and cloned into His-tagged fusion constructs. Recombinant Rrp46/CRN-5 proteins were over-expressed in *E. coli* by IPTG induction and purified by chromatographic methods. Crude cell extracts were first loaded onto a TALON resin affinity column (BD Biosciences) followed by a gel filtration chromatography column (Superdex 200, Pharmacia). The final purified pattern of gel filtration showed single peak of each protein (Figure 3-1). The His-tagged oRrp46 and hRrp46 were purified to a homogeneity of greater than 98%, whereas CRN-5 was less homogeneous with a partial population of cross-linked dimers as shown by SDS-PAGE in a reduced condition (Figure 3-1). We have also tried to make

different expression constructs of CRN-5, or treat CRN-5 with and without the addition of different reducing agents (β-mercaptoethanol, DTT and TCEP) ranging from 1 to 10 mM and found no difference in the purification steps and SDS-PAGE analysis. Mass spectrometry verified the correct molecular weight of each protein (data not shown, theoretical molecular weights for the recombinant proteins: 26,974 Dalton for oRrp46, 24,988 Dalton for CRN-5, and 27,412 Dalton for hRrp46). The three proteins share high sequence identity, 35% between hRrp46 and oRrp46, 31% between hRrp46 and CRN-5, and 28% between oRrp46 and CRN-5 (see Figure 1-6).

3.3 Recombinant purified CRN-5/Rrp46 proteins form stable homodimer in vitro.

In hexameric exosome complex, Rrp46 forms stable heterodimer with Rrp43 and shares interaction interface with Rrp45. In order to determine the oligomeric state of these three recombinant purified proteins, we combined size-exclusion chromatography, dynamic light scattering (DLS) and analytical ultracentrifugation (AUC) to analyze proteins in solution condition. The three purified proteins, CRN-5, oRrp46 and hRrp46, eluted with a size between 44 kD to 75 kD in size-exclusion chromatography under reduced conditions (1 mM β-mercaptoethanol) (Figure 3-1). The molecular weights of the three proteins estimated by dynamic light scattering (DLS) under reduced conditions (1 mM DTT) were also in the range of 42 to 59 kD (Figure 3-2). The molecular weights of hRrp46 and CRN-5 proteins estimated from sedimentation velocity analysis by analytical ultracentrifugation (AUC) were 47.0 kD and 42.6 kD, respectively (Figure 3-3). With all of these data, we suggest that the recombinant proteins were homodimers with molecular weights of ~50 kD.

3.4 Endogenous Rrp46 forms a separated dimer in addition to associating with a protein complex in vivo.

To further verify that Rrp46 forms homodimers in a cellular environment, endogenous Rrp46 in the total cell extracts of human 293T cells and rice callus were blotted using antibodies against hRrp46 and oRrp46 after fractionated by size-exclusion chromatography (Figure 3-4). Two populations of hRrp46 were observed at different elution volumes with or without the addition of the reducing agent (1 mM β-mercaptoethanol): the first peak eluted at 45~60 ml indicating a high-molecular-weight complex and the second peak appeared at 80-85 ml indicating a mixture of a dimer and a monomer. The cell extract of rice callus gave similar results that oRrp46 migrated as a large size complex and a smaller size dimer. As a control, the 293T cell extract eluted from gel filtration fractionation was also blotted with antibodies against hRrp42, one of the six RNase PH family proteins in the exosome core. The Western blot displayed in Figure 3-4 shows that hRrp42 only eluted in a complex with a molecular weight greater than 158 kD. The complex identified by anti-hRrp42 overlapped with the complex indicated by probing with anti-hRrp46, suggesting that both proteins were likely associated with the same complex, the exosome. This result is in consistent with the previous result in the reconstitution of human exosome in which a monodisperse peak with a molecular weight of ~400 kD and a smaller size peak were observed with anti-hRrp46 in the gel filtration under low salt conditions (Liu et al., 2006). Meanwhile, endogenous AtRrp41 was only found in a large complex in *Arabidopsis* cells by glycerol gradient sedimentation (Chekanova et al., 2000). In summary, these results suggest that the exosome component protein hRrp42 is associated with a protein complex, but it does not form a monomer or a dimer in cells.

On the other hand, the endogenous Rrp46 is associated with a protein complex and it also forms a separate dimer in a cellular environment.

3.5 CRN-5 and Rrp46 are DNA binding proteins, but only rice Rrp46 is a RNA binding protein.

The three Rrp46 proteins were then incubated separately with DNA and RNA for gel retardation assays to determine their DNA- and RNA-binding ability (Figure 3-5). The mobility of a ^{32}P-labeled 20-bp DNA was retarded by Rrp46/CRN-5, showing that the three recombinant proteins all bound to the double-stranded DNA (Figure 3-5A). hRrp46 seems to show stronger binding ability against 20-bp dsDNA than two other proteins. When incubated with *in vitro*-transcribed 2.3 kb ssRNA, only oRrp46 shows ssRNA-binding activity (Figure 3-5B). In contrast, hRrp46, CRN-5 and hRrp42 could not bind to ssRNA. The retarded smears resulted from oRrp46 binding to the 2.3 kb RNA further suggests that multiple oRrp46 in high concentrations were bound to the large-size ssRNA, likely without sequence specificity, to induce the observable shifts.

3.6 Dimeric rice oRrp46 shows metal-dependent DNase activity.

Since these three Rrp46/CRN-5 proteins have DNA-binding activity, in combination with the inspiration of that CRN-5 may play a role in apoptotic DNA degradation. We wonder these RNase PH proteins have DNase activity. 309-bp dsDNA was PCR amplified from pET-22b vector and then purified as substrate for DNase assay. Only oRrp46 degraded a linear 309-bp DNA, while hRrp46 and CRN-5 had no detectable DNase activity with a protein concentration of 1 μM in the time-course experiments (Figure 3-6A), suggesting that the recombinant proteins hRrp46 and CRN-5 (and a negative control of RNase T) had either no or very low DNase activites in

the *in vitro* condition. Divalent metal ions, preferably Ca^{2+} over Mg^{2+}, but not phosphate ions, were required for the DNase activity of oRrp46 (Figure 3-6B), suggesting that oRrp46 was a hydrolase rather than a phosphorylase in the digestion of dsDNA. Moreover, oRrp46 cleaved the plasmid DNA, as in contrast to an exonuclease TREX2, suggesting that oRrp46 has endonucleolytic DNase activity (Figure 3-6C). The bacterial RNase PH has been shown to bind DNA previously (Jensen et al., 1992), and for the first of time, we show here that an RNase PH family protein oRrp46 has metal-dependent hydrolytic DNase activity.

3.7 Rice oRrp46 shows typical RNase PH activity.

To determine the RNA-cleavage activity, oRrp46, hRrp46 and CRN-5 were incubated with *in vitro*-transcribed 2.3 kb ssRNA for RNA cleavage assays. Figure 3-7A shows that oRrp46 had RNase activity against ssRNA. In contrast, CRN-5 and hRrp46 could not digest ssRNA.

To further confirm that oRrp46 is a phosphorylase, RNase assays were performed in the presence or absence of phosphate ions. oRrp46 digested a 20-nucleotide ssRNA only in the presence of both Mg^{2+} ions and phosphate ions (Figure 3-7B). Moreover, using an *in vitro*-transcribed [α-^{32}P]ATP-incorporated single-stranded RNA as substrates, oRrp46 cleaved ssRNA into ADP but not AMP (Figure 3-7C), further confirming that oRrp46 was a phosphorolytic RNase.

Altogether, these results suggest that rice oRrp46 is not only a hydrolytic DNase but also a phosphorolytic RNase, whereas the human hRrp46 and the worm homologue CRN-5, are only capable of binding to DNA but have neither DNase nor RNase activity.

3.8 Crystallization of CRN-5 and rice oRrp46 proteins.

To elucidate the molecular basis of oRrp46 and CRN-5 in domain assembly and nucleic acid cleavage activity, we crystallized the two proteins for three-dimensional structural determination. A number of conditions were also screened for the co-crystallization of oRrp46 with metal ions, phosphates, RNA and DNA substrates however, only the apo-form of oRro46 was crystallized. All the crystals were grown by hanging-drop vapor diffusion methods, by mixing 1-μl of protein solution with 1-μl of reservoir solution. oRrp46 (7.5 mg/ml) crystals were grown from a reservoir solution containing 0.2 M sodium malonate (pH 7.0) and 20% PEG3350 (Figure 3-8A). The CRN-5 (30 mg/ml) crystals were grown from a reservoir solution containing 0.1 M Tris-HCl (pH 8.0), 0.2 M NaCl and 25% PEG3350 (Figure 3-8B). Both crystals were grown under room temperature for days to weeks.

oRrp46 crystallized in the trigonal space group $P3_1$ as twin crystals with a twin factor of 0.5, and the twin operation of the Miller index was (h,-h-k,-l). There are three molecules per asymmetric unit, diffracting X-rays to a resolution of 2.0 Å. Whereas, CRN-5 crystallized in the monoclinic space group $P2_1$ with two molecules per asymmetric unit, diffracting X-rays to a resolution of only 3.9 Å (Table 3). Both structures were solved by molecular replacement using the crystal structure of human Rrp46 (PDB accession code 2NN6, chain D) as the search model. The statistics for X-ray diffraction and structural refinement are listed in Table 3.

3.9 Overall structure of dimeric CRN-5 and momomeric rice oRrp46 proteins.

oRrp46 was a dimer in solution; however, the three molecules in the asymmetric unit shared little contact area with buried interfaces less than 300 $Å^2$ for each subunit (Figure 3-9). To confirm the oligomeric state in the crystals, we found that oRrp46 was

a monomer in the crystallization condition with a buffer solution containing 5% PEG3350 using gel filtration assays (see the elution profile marked with oRrp46/PEG in Figure 3-10A). The human hRrp46 in the reconstituted six-subunit exosome complex also migrated as a monomer in the gel filtration analysis under low salt conditions, suggesting that hRrp46 dimers may be dissociated into monomers at a low ionic-strength condition (Liu et al., 2006). Moreover, we found that oRrp46 lost its DNase activity in the presence of 20% PEG3350, indicating that the dimeric conformation is important for the DNase activity (see Figure 3-10B). Therefore oRrp46 was crystallized in a monomeric form, dissociated by PEG3350. The final model had an R-factor/R-free of 0.169/0.235 for 54,728/2,776 reflections at a resolution of 2.0 Å.

The monomeric oRrp46 adopts a β-α-β-α folding and shares a similar structure to other RNase PH exonucleases (Figure 3-11A). Superposition of oRrp46 onto hRrp46 by the secondary-structure based method gave an RMSD of 1.29 Å over 187 C_α atoms. Superposition of oRrp46 onto archaeal Rrp41-Rrp42 dimer (PDB accession code: 2JEA) gave an RMSD of 1.32 Å over 202 C_α atoms against the active Rrp41, and 1.49 Å over 197 C_α atoms against the inactive Rrp42 (Figure 3-11B). This result suggests that oRrp46 shares a similar overall structure to other RNase PH family proteins with or without RNase activity.

To understand how Rrp46 monomers associate into a dimer, CRN-5 was crystallized in the conditions favoring homodimer formation. The resolution of the CRN-5 structure was only 3.9 Å, but this was sufficient to reveal the overall folding and dimeric assembly. The crystal structure of the dimeric CRN-5 is shown in Figure 3-12A, with a major interface contributed to by two antiparallel β-strands (residues 170-176) (see Figure 1-5, β10). A hydrophobic area formed by the residues FIQL (180-183) of

the α4 helix also stabilized the dimeric interface.

The CRN-5 structure is the first homodimeric structure observed in the RNase PH family proteins, the rest of which all crystallized in trimeric or hexameric forms with six RNase PH domains forming a ring-like structure, including human exosome (Liu et al., 2006), archaeal exosome (Buttner et al., 2005; Lorentzen and Conti, 2005; Lorentzen et al., 2005; Navarro et al., 2008), bacterial PNPase (Shi et al., 2008; Symmons et al., 2000) and RNase PH (Harlow et al., 2004a; Ishii et al., 2003a). Superposition of CRN-5 dimer over hRrp46-hRrp43 gave an RMSD of 3.05 Å over 273 C_α atoms, whereas superposition of CRN-5 dimer onto archaeal Rrp41-Rrp42 dimer (PDB accession code: 2JEA) gave an RMSD of 3.02 Å over 279 C_α atoms (Figure 3-12B). This result suggests that the dimeric assembly mode of CRN-5 is similar to the one that exists between hRrp43 and hRrp46 in the human exosome, and to the one between Rrp41 and Rrp42 in archaeal exosomes.

3.10 A metal binding residue is conserved in RNase PH family protein and critical to DNase activity of rice oRrp46.

oRrp46 has both DNase and RNase activity, so the next question that arose was where the substrate-binding and active sites are in the dimeric oRrp46. The active residues of phosphorolytic RNase PH domain have been well studied in archaeal exosomes (Buttner et al., 2005; Lorentzen and Conti, 2005; Navarro et al., 2008). One acidic residue (D182 in *S. sulfataricus*, D180 in *P. abyssi*) is critical for the RNase activity of archaeal Rrp41 and this acidic residue is conserved in both active and inactive RNase PH proteins, including D486 of PNPase, E174 of hRrp46, E219 of hRrp42, D180 of PaRrp41 and E160 of oRrp46 (Figure 3-13A). The recent crystal

structure analysis of the *E. coli* PNPase bound to a manganese further suggests that this conserved acidic residue (D486) is bound to the metal ion, responsible for stabilizing the transition state (Nurmohamed et al., 2009). Superposition of the structure of oRrp46 with all of these RNase PH enzymes showed that E160 in oRrp46 fitted well with the conserved acidic residues (marked by an arrow in Figure 3-13B). We therefore mutated E160 to determine whether this residue is a catalytic residue in oRrp46. As a result, the purified oRrp46 E160Q lost most of its DNase activity in digesting a linear 309-bp dsDNA (see Figure 3-15A); however the mutant only lost partial activity in digesting a 20-mer ssRNA (Figure 3-15B). This result suggests that E160 plays a more important role in catalyzing the hydrolytic cleavage of DNA, and it plays a less critical role in the phosphorolytic cleavage of RNA.

3.11 Substrate binding residues are variable in RNase PH family protein and important to both RNase and DNase activity of rice oRrp46.

To determine the residues involved in nucleic acid binding, we compared the crystal structures of oRrp46 with those of active archaeal Rrp41 (PDB accession code: 2PO1, chain B) and human hRrp46 (PDB accession code: 2NN6, chain D). A five-nucleotide RNA substrate bound in the structure of *P. abyssi* Rrp41-RNA complex reveals two important basic residues, R96 and R97, involved in RNA binding (circled in Figure 3-14) (Navarro et al., 2008). These two basic residues are missing in the inactive hRrp46 (grey, V89 and A90) and hRrp42 (yellow, D100 and L101), suggesting that the loss of RNase activity is likely a result of the loss of RNA binding activity. In oRrp46 a polar (Q76) and a basic (K75) residue are located at the corresponding RNA-binding site, and may play a similarly important role in RNA binding. To verify our hypothesis, we

constructed a double mutant of oRrp46, K75E/Q76E, to test its RNA-binding and cleavage activity. This oRrp46 mutant (K75E/Q76E) almost completely lost its DNA- and RNA-binding activity in gel retardation assays (Figure 3-15C and 3-15D). The DNase and RNase activity were also abolished, compared to the wild-type oRrp46 (Figure 3-15A and 3-15B). Therefore, K75 and Q76 of oRrp46 are indeed involved in RNA and DNA binding. Impairment of the substrate binding ability of oRrp46 results in the loss of its nuclease activity.

3.12 CRN-5 interacts with another apoptotic nuclease CRN-4 and enhances CRN-4's DNase activity.

CRN-5 was identified as a cell death-related nuclease involved in DNA fragmentation during apoptosis in *C. elegans* (Parrish and Xue, 2003a). However, here we show that CRN-5 only binds to DNA without detectable DNase activity. It was therefore puzzling how CRN-5 is involved in DNA fragmentation. It has been shown previously that CRN-5 is a component of a protein complex, the degradeosome, interacting with CPS-6, CRN-4, CRN-1 and CYP-13 in GST-pull-down assays (Parrish and Xue, 2003a). To further clarify the role of CRN-5 in DNA degradation, we tested its interaction with CRN-4, a fully characterized DEDD family apoptotic nuclease with both DNase and RNase activity (Hsiao et al., 2009). We confirmed that His-tagged dimeric CRN-5 interacted directly with dimeric CRN-4 by His-tag pull-down assays (see Figure 3-16A) (Parrish and Xue, 2003a). Moreover, the DNase activity of CRN-4 was enhanced by the presence of CRN-5 compared to that of CRN-4 alone (6.5% DNA remained, compared to 13% DNA remained with CRN-4 alone; Figure 3-16B). This result suggests that CRN-5 promotes CRN-4's DNase activity and these two proteins act

cooperatively in DNA degradation.

4. DISCUSSION

4.1. RNA binding residues are critical for the enzyme activity of RNase PH proteins.

RNase PH family proteins are a group of fascinating enzymes, sharing similar sequences and structures, but they have evolved differently with either retained or lost RNase activity (Symmons et al., 2002). They can be grouped into active RNases, which include RNase PH, the second PH domain of PNPase, archaeal Rrp41, plant Rrp41 and oRrp46; and inactive RNases, including the first PH domain of PNPase, archaeal Rrp42 and all the human and yeast RNase PH proteins in exosomes. The structural basis of an active versus an inactive RNase PH enzyme in RNA cleavage is still under discussion. Previous studies have focused on the comparison of the conserved general-acid residue and the varied phosphate binding residues among the RNase PH family proteins (Buttner et al., 2005; Lorentzen and Conti, 2005; Navarro et al., 2008).

Here we identify a quite significant feature in RNase PH family proteins that differentiates an active enzyme from an inactive one. We found that the active oRrp46 has a positively-charged region located at the RNA entry site (due to "strong RNA-binding residues" shown in Figure 3-14), which may facilitate RNA binding (marked by a red circle in Figure 3-17). A similar positively-charged RNA-binding region can be observed on the active enzymes of archaeal Rrp41 (PaRrp41) and the second domain of PNPase (PNPase_RNase PH II). On the contrary, the surface of the corresponding regions on the inactive enzymes, including archaeal Rrp42 (PaRrp42), the first domain of PNPase (PNPase_RNase PH I) and human Rrp46, are neutral or even acidic, and thus not suitable for RNA binding (marked by a green circle in Figure 8). The loss of nucleic acid binding ability in the oRrp46 K75E/Q76E mutant resulted in the loss of its RNA cleavage activity, further supporting this suggestion that the ability

to bind substrate is closely related to the nuclease activity of an RNase PH enzyme. This observation is true for all the RNase PH proteins with known structures, except for the inactive human Rrp41, which has suitable residues for the role of general acid and phosphate binding, and also appropriate residues for RNA binding (Lorentzen and Conti, 2005). Therefore we conclude that possessing the correct RNA-binding residues at the entry site of an RNase PH protein is a necessary but not sufficient condition for efficient RNase activity.

Archaeal Rrp41 alone shows no RNase activity in the absence of Rrp42 (Lorentzen et al., 2005). Not only the critical substrate binding residues on Rrp41, but also the Rrp41-Rrp42 interface offers essential binding packet for RNA substrate (Lorentzen and Conti, 2005; Navarro et al., 2008). When dimeric rice oRrp46 dissociated into monomer, it also lost its DNase activity (Figure 3-10). This suggests that the formation of homodimeric rice oRrp46, or the interface of this dimer may also plays a important role in DNA binding and catalysis.

4.2 Dual roles of Rrp46 in RNA turnover and DNA degradation.

Our biochemical and structural analyses demonstrate that the eukaryotic exosomal component proteins, including hRrp46 and oRrp46, form a stable homodimer *in vivo* and *in vitro*. The homodimeric rice oRrp46 shows, for the first time, both a hydrolytic DNase and a phosphorolytic RNase activity. On the other hand, the nematode Rrp46 (CRN-5) and human hRrp46 had no detectable DNase and RNase activities. It has been shown that AtRrp41 from *Arabidopsis thaliana* displays a processive phosphorolytic exoribonuclease activity, and endogenous AtRrp41 was only found in a large complex in *Arabidopsis* cells by glycerol gradient sedimentation (Chekanova et al., 2000). Our

results show, without forming an exosome complex, that homodimeric oRrp46 alone is also an active phosphorolytic RNase. The RNase activity of oRrp46 can be abolished by substrate binding site (K75 and Q76) mutation, excluding the possibility of contamination by *E. coli* enzymes during protein preparation. This result thus shows that eukaryotic exosome core complexes have evolved distinctive ways of degrading RNA, as some of the plant exosome RNase PH component proteins do have RNase activities, compared to the yeast and human exosomal proteins which have no detectable activity.

Rrp46/CRN-5 is also a candidate for apoptotic DNA degradation in *C. elegans* (Parrish and Xue, 2003a). Here we show that rice oRrp46 indeed has DNase activity, and *C. elegans* CRN-5 enhances the DNase activity of CRN-4. These results provide new lines of evidence to support the involvement of Rrp46 in apoptotic nucleosomal degradation. Although CRN-5 only increases the DNase activity of CRN-4 slightly *in vitro*, it is likely that various apoptotic nucleases in the degradeosome complex, including CPS-6, CRN-1, CRN-3, CRN-4, CRN-5 and CYP-13, work together and increase the efficiency of DNA degradation with a synergistic effect in cellular environments. Another exosome component protein, CRN-3, a homologue of human PM-Scl100 and yeast Rrp6, is also implicated in the degradeosome and is suggested to be involved in DNA degradation during apoptosis (Parrish and Xue, 2003a). Therefore, CRN-5 is not the only exosome component protein that is identified as a player in DNA fragmentation during apoptosis.

In addition to its roles in promoting cell killing, apoptotic DNA degradation may play an important role in higher organisms to remove highly antigenic DNA or nucleosomes from apoptotic cells to prevent them from eliciting autoimmune responses. Interestingly, auto-antibodies against both PM-Scl100 and hRrp46 are often identified in

the patients with autoimmune diseases (Bluthner and Bautz, 1992; Brouwer et al., 2002; Ge et al., 1992; Reichlin et al., 1984). Loss or reduction of DNase activity of several nucleases has been shown to link to a number of autoimmune diseases, such as DNase I associated with systemic lupus erythmatosus (Napirei et al., 2000; Yasutomo et al., 2001), and DNase II associated with rheumatoid arthritis (Kawane et al., 2006). It is suggested that the DNA escaped from degradation during program cell death elicits autoimmune responses, however, the underlying mechanisms and signaling events that regulate innate immune responses to extracellular and cytosolic undigested DNA are still elusive (Green et al., 2009; Okabe et al., 2009). The finding of auto-antibodies of hRrp46 and PM-Scl100 in autoimmune diseases hints a link between the two exosome component proteins and DNA degradation.

A search in the cancer database further shows that hRrp46 is upregulated in various cancer tissues, including eye, lung, placenta and skin cancers (see Figure 3-18) (Krizman et al., 1999). This upregulation trend is however not observed for other exosomal RNase PH proteins, further suggesting that hRrp46 may play a function other than RNA turnover and processing. In summary, our results strongly support the notion that Rrp46/CRN-5 forms a homodimer, participating in DNA degradation in cell death. Rrp46 likely switches its role and plays dual functions between life and death. Based on these biochemical, cellular, structural and mutational results, we suggest that Rrp46 is not only an exosome component protein participating in RNA degradation and processing, but that it also forms a homodimer involved in DNA degradation in apoptosis. This finding therefore opens a new direction for the future study of hRrp46 to uncover its link to autoimmune diseases and cancer.

4.3 C. elegans uses functional-known proteins to accomplish apoptotic DNA degradation.

Most of the apoptotic nucleases in *C. elegans* list in Table 2 have normal cellular functions that are critical for cell survival. For example, DCR-1/Dicer is for gene silencing in RNAi (Nakagawa et al., 2010); CRN-1/FEN-1 is important for DNA repair and replication (Parrish et al., 2003); cyclophilins are involved in protein folding (Andreeva et al., 1999; Mi et al., 1996); AIF is essential for mitochondrial respiration (Vahsen et al., 2004); and CRN-3 and CRN-5 are involved in RNA processing and degradation (Brouwer et al., 2001). During apoptosis, these proteins likely switch their roles to execute chromosomal DNA degradation. The regulation for switching the role in a cellular environment is another interesting issue.

DCR-1/Dicer is cleaved by caspase-3 to become a functional apoptotic DNase. Translocation of AIF and EndoG from mitochondria to nucleus is the first step for their pro-apoptotic function. Besides phosphorolytic RNase activity, homo-dimeric plant Rrp46 (rice oRrp46) has in vitro hydrolytic DNase activity, implying that it might function as an apoptotic DNase. How CRNs can be gathered to form a degradeosome complex may be the most important regulation mechanism for switching the normal function of CRN proteins into apoptotic DNA fragmentation. Knowing the detail of these mechanisms will help us to understand about how a cell works in life and death, and to facilitate the pro-apoptotic drug design in specifically eliminating cancer cells without affecting normal cellular functions.

5. FUTURE WORKS

5.1 The DNA hydrolysis mechanism of oRrp46.

Rice oRrp46 digests RNA substrate through a mechanism of phosphorolysis in the

requirement of both divalent metal ion and inorganic phosphate (Figure 3-7B). On the contrary, it degrades DNA substrates through a mechanism of hydrolysis in the presence of divalent metal ion (Figure 3-6B). The results of mutagenesis analysis also showed that E160 plays a crucial role in DNase activity, but not in RNase activity of rice oRrp46 (Figure 3-15A and B). These data suggest that rice oRrp46 catalyzes DNA and RNA degradation through different molecular mechanisms. To understand the detail mechanism of how an RNase PH protein (rice oRrp46) binds to and digests DNA substrates, several analyses can be further performed :

a. The binding stoichiometry between rice oRrp46 and DNA substrate can be determined by *isothermal titration calorimetry* (ITC) analysis.

b. The binding preference in nucleotide composition of DNA substrate can be determined by electrophoretic mobility shift assay (EMSA) and filter binding assay.

c. oRrp46 can be co-crystallized with DNA. We can observe the detail binding and catalytic pattern through co-crystal structure.

In comparison with the co-crystal structures of archaeal exosome-RNA complexes, we can tell the differences between DNA and RNA digestion mechanisms of an RNase PH protein.

5.2 Critical roles of substrate binding residues in RNase PH proteins

The K75 and Q76 of rice oRrp46 are relevant to R96 and R97 of archaeal PabRrp41 in substrate binding (Figure 3-14). The mutagenesis assay also supported the two residues (K75 and Q76) are important in substrate binding of rice oRrp46 (Figure 3-15C and D).We can further demonstrate whether these substrate binding residues play an important role in evolution of active and inactive RNase PH proteins by double-mutating V89 and A90 of human hRrp46 (Figure 3-14) to basic residues. If this

mutation recovers the substrate binding ability of human hRrp46, then we can prove the importance of substrate binding in divergent evolution of RNase PH proteins.

5.3 Cooperation between CRN proteins.

CRN proteins together with CPS-6 interact with each other *in vitro* and could complex into large degradeosome during apoptosis (Figure1-4). We further confirmed that CRN-5 directly interacts with CRN-4 protein and enhances CRN-4's DNase activity (Figure 3-16). To elucidate how CRN-5 interacts with other CRN proteins and CPS-6, we may use co-expressing system to get the stable complex of CRN proteins. By gel filtration analysis, the interaction stoichiometry of CRNs can be estimated according to the molecular weight of complex. Enzymatic activity of different combination of CRN proteins can be tested to see whether there is a cooperative effect between each other, and it reaches the maximum activity when formation of the degradeosome complex. With recombinant purified CRN complex, co-crystallization can then be performed to determine the interaction interface between proteins. These CRN proteins function in different physiological environments and with various enzymatic characteristics in normal cell. Understanding the molecular basis of their interaction during apoptosis by structural biology methods can clarify the regulative mechanism of degradeosome complex formation.

Table 1. Exosome components and cofactors (Schmid and Jensen, 2008)**.**

	Domains	Archaea[b]	*S. cerevisiae*[c]	Loc[d]	Human[c]	Loc[d]
Exosome core	RNasePH	Rrp41	Rrp41p (Ski6p)	n+c	hRrp41 (hSki6; EXOS4)	n+c
		Rrp42	Rrp42p	n+c	hRrp42 (EXOS7)	n+c
		(Rrp41)	Rrp46p	n+c	hRrp46 (EXOS5)	n+c
		(Rrp42)	Rrp43p	n+c	hRrp43 (OIP2; EXOS8)	n+c
		(Rrp41)	Mtr3p	n+c	hMtr3 (EXOS6)	n+c
		(Rrp42)	Rrp45p	n+c	hRrp45 (Pm/Scl-75; EXOS9)	n+c
	S1 and KH domains	Rrp4	Rrp4p	n+c	hRrp4 (EXOS2)	n+c
		(Rrp4)	Rrp40p	n+c	hRrp40 (EXOS3)	n+c
		Csl4	Csl4p	n+c	hCsl4 (EXOS1)	n+c
Exonuclease	RNase II	–	Rrp44p (Dis3p)	n+c	hRrp44 (hDis3)	n+c
	RNase D	–	Rrp6p	n	hRrp6 (PM/Scl-100; EXOS10)	n+c
Co-factors	RNA binding	–	Rrp47p (Lrp1p)	n	C1D (hRrp47)	n
	RNA binding	–	Mpp6p	n	Mpp6	n
TRAMP	Poly(A) polymerase	–	Trf4p (Pap2p)	n	?PAPD5 and POLS	?
	Poly(A) polymerase	–	Trf5p	n	?PAPD5 and POLS	?
	RNA binding	–	Air1p	n	?ZCHC7	?
	RNA binding	–	Air2p	n	?ZCHC7	?
	DExH RNA helicase	–	Mtr4p (Dob1p)	n	hMtr4 (Skiv2L)[e]	n+c
Nrd1–Nab3 complex	RNA binding and CTD binding	–	Nrd1p	n	?	?
	RNA binding	–	Nab3p	n	?	?
	Helicase	–	Sen1p	n	Senataxin	?
SKI complex	DExH RNA helicase	–	Ski2p	c	hMtr4 (Skiv2L)[e]	n+c
		–	Ski3p	c	hSki3	n+c
		–	Ski8p	c	hSki8	n+c
Ski7	EF1α-like	–	Ski7p	c	?	?

[a]Abbreviations: Air, arginine-methyltransferase-interacting RING-finger protein; CTD,C-terminal domain of RNA polymerase II; Dob1, dependent on eIF4B; EXOS, exosome component; OIP2, Opa-interacting protein 2; Pm-Scl, polymyositis- scleroderma; PAPD5, PAP-associated-domain- containing 2; POLS, DNA polymerase sigma; Sen1, splicing endonuclease 5; Skiv2L, superkiller viralicidic activity 2-like; ZCHC7, zinc-finger CCHC-domain-containing protein 7.

[b]Archaeal homologs of the eukaryotic exosome subunits. Note that eukaryotes contain three distinct Rrp41, Rrp42 and 2 Rrp4 homologs. '_' indicates that functional homologs are unlikely to exist.

[c]Yeast and human exosome components and co-factors. Entries in parentheses indicate alternative protein names. '?' indicates that sequence homologs cannot be identified or have not yet been functionally analyzed.

[d]Nuclear (n) or cytoplasmic (c) location of yeast and human factors.

[e]The human genome encodes only one homolog, called hMtr4 or Skiv2L, for the related yeast proteins Mtr4 and Ski2. hMtr4/Skiv2L is 55% and 34% identical with Mtr4 and Ski2, respectively.

Table 2. Apoptotic nucleases in *C. elegans* and their homologues in human.

C. elegans **Cell death-related protein**	**Human homolog**
DCR-1	Dicer
CPS-6	EndoG
CRN-1	FEN-1
CRN-2	TatD nuclease
CRN-3	hRrp6/PM/Scl-100
CRN-4	3'-5' exonuclease
CRN-5	Rrp46
CRN-6	Type II DNase
Cyp-13	Cyclophilin E
WAH-1	AIF

Table 3. Exosomal RNase PH proteins in *C. elegans*

Human	*C. elegans* (identity,%)
hRrp41	exos-4.1 (B0564.1a)[a] (43%)
hRrp46	CRN-5 (C14A4.5)(31%)
hMtr3	exos-4.2 (Y6D11A.1.1) (25%)
hRrp42	exos-7 (F31D4.1) (32%)
hRrp43	exos-8 (F41G3.14) (23%)
hRrp45	exos-9 (F37C12.13a.1) (36%)

[a]sequence name in WormBase (http://www.wormbase.org/)

Table 4. X-ray data collection and refinement statistics for rice oRrp46 and *C. elegans* CRN-5

Data collection statistics	**oRrp46**	**CRN-5**
Space group	$P3_1$	$P2_1$
Cell dimensions (Å/ degree)	a = 111.61 α = 90	a = 61.92 α = 90
	b = 111.61 β = 90	b = 44.83 β = 100.67
	c = 57.70 γ = 120	c = 65.58 γ = 90
Wavelength (Å)	1.00	1.00
Resolution (Å)	50.00- 2.00	50.00- 3.90
	(2.07- 2.00)[1]	(4.04- 3.90)[1]
Observed reflections	185,470	9,991
Unique reflections	55,506	3,235
Completeness (%)	99.8 (99.7)	97.7 (91.3)
<I>/<σI>	21.65 (3.16)	14.06 (5.28)
Rsym[2](%)	6.50 (35.40)	9.1 (26.70)
Refinement statistics		
Resolution range (Å)	50.00- 2.00	50.00- 3.90
Reflections (working/ test)	54,782/ 2,776	3,217/ 227
R-factor/ R-free (%)	16.9/ 23.5	30.7/ 35.6
Number of atoms (protein/water)	4,687/ 416	2,576/ 0
Average B-factor (Å^2)	26.1	87.9
RMS deviations	0.006/ 1.090	0.005/ 0.989
(bond length (Å)/ bond angle (degree))		
Ramachandran plot (%)		
Most favored/ Additional allowed/ Generously allowed/ Disallowed	89.2/ 10.6/ 0.2/ 0.0	66.5/ 28.2/ 3.9 /1.4

[1]Highest-resolution shell is shown in parentheses.

[2]Rsym = $\sum hkl \sum i \mid Ii(hkl) - \langle I(hkl) \rangle \mid / Ii(hkl)$.

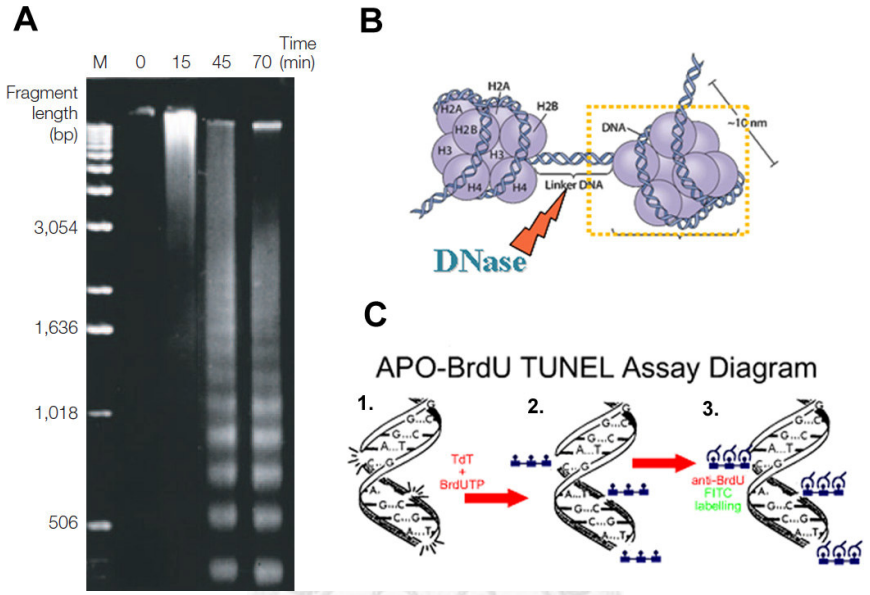

Figure 1-1. Apoptotic DNA fragmentation and principles of TUNEL assay.

(A) The DNA forms a low molecular weight (LMW) oligonucleosomal ladder when isolated HeLa nuclei undergo apoptotisis (Samejima and Earnshaw, 2005). (B) The ladder is a consequence of the cleavage (orange thunder) of chromatin by endonucleases that target the linker DNA between the nucleosomes. (C) Terminal deoxynucleotidyl transferase-mediated dUTP nick end labeling (TUNEL) is a method for detecting DNA fragmentation by labeling the terminal end of nucleic acids (www.phnxflow.com/ apobrdu.html) **1.** DNA strand breaks caused by endonucleases produced by apoptosis process. **2.** Add BrdUTPs to 3'-OH DNA strand breaks using TdT enzyme as catalyst. **3.** Fluorescenated antibody labeling of BrdUTP attached to 3'-OH DNA strand breaks.

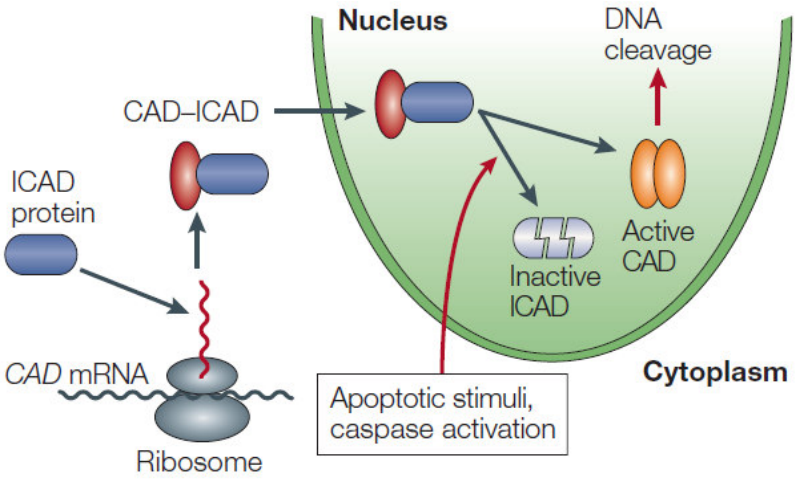

Figure 1-2. Regulation of caspase-activated DNase (CAD) by its inhibitor (Samejima and Earnshaw, 2005)**.**

ICAD (inhibitor of CAD; also known as DFF45) functions as a chaperone for CAD (caspase-activated DNase; also known as DFF40 (DNA fragmentation factor, 40kDa) and CPAN (caspase-activated nuclease)), helping the peptide to fold as it is translated on the ribosome. ICAD then remains bound and inhibits CAD activity as the complex transfers to the nucleus. When cells undergo apoptosis, caspases cleave ICAD, liberating active CAD.

A

Gene	Strain Treated by RNAi: N2 TUNEL	n
	2.3 ± 0.5	16
cps-6	19.9 ± 0.5	15
nuc-1	30.9 ± 0.7	25
crn-1	11.3 ± 0.7	15
crn-2	13.3 ± 0.8	16
crn-3	11.8 ± 0.8	16
crn-4	12.2 ± 0.9	16
crn-5	13.9 ± 0.9	13
crn-6	11.8 ± 0.7	17
cyp-13	16.8 ± 0.8	15

B

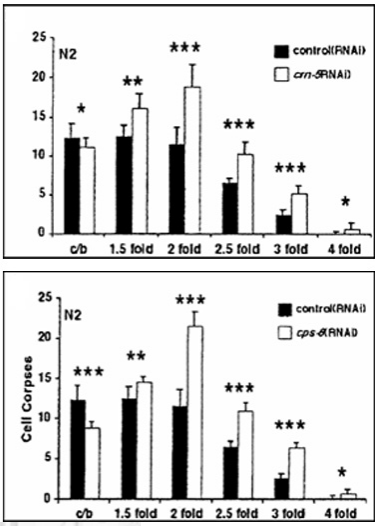

Figure 1-3. RNAi knock-down of *crn-5* in *C.elegans* embryo (Parrish and Xue, 2003b)**.**

(A) RNAi mediated depletion of *crn-5* gene results in accumulation of TUNEL- stained nuclei in RNAi treated embryos. (B) RNAi knock-down of *crn-5* (up) delayed appearance of embryonic cell corpses during development which is similar to that of *cps-6* (bottom).

A

^{35}S-proteins	GST	CPS-6	NUC-1	CRN-1	CRN-3	CRN-4	CRN-5	CRN-6	CYP-13
	GST-fusion proteins								
Luciferase	-	-	-	-	-	-	-	-	-
CPS-6	-	+	-	++	-	++	+	-	+
NUC-1	-	-	-	-	-	-	-	-	-
CRN-1	+	++	+	+	+	++	+	+	++
CRN-2	-	-	-	-	-	-	-	-	-
CRN-3	+	+	+	+	++	+	++	+	+
CRN-4	-	+	+	+	-	++	++	-	++
CRN-5	-	+	+	-	-	++	++	-	++
CRN-6	-	-	-	-	-	-	-	-	-
CYP-13	-	++	-	+	-	++	++	-	++

B

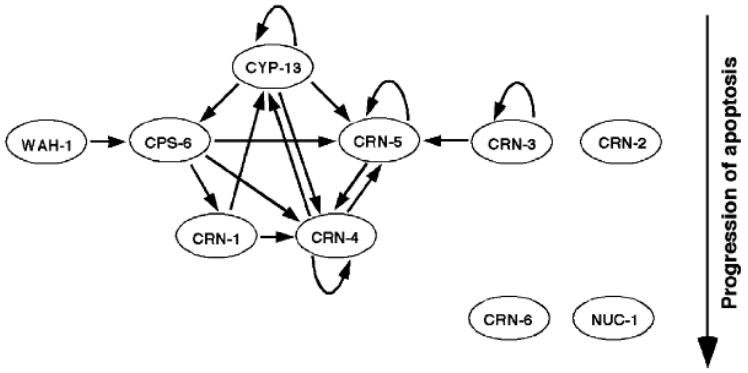

Figure 1-4. Analysis of in vitro interactions among *C. elegans* apoptotic nucleases (Parrish and Xue, 2003b).

(A) Summary of in vitro interactions among CPS-6, NUC-1, CPY-13, and six CRN proteins. Interactions between proteins were examined using GST fusion protein pull-down assays. "-" indicates no detectable binding, "+" indicates an interaction consistently observed above background levels, and "++" indicates a strong interaction. (B) Interaction map for nucleases involved in apoptotic DNA degradation in *C. elegans*. An arrow indicates an interaction between a GST-fusion protein (pointed by the arrow) and a ^{35}S-Methionine-labeled protein.

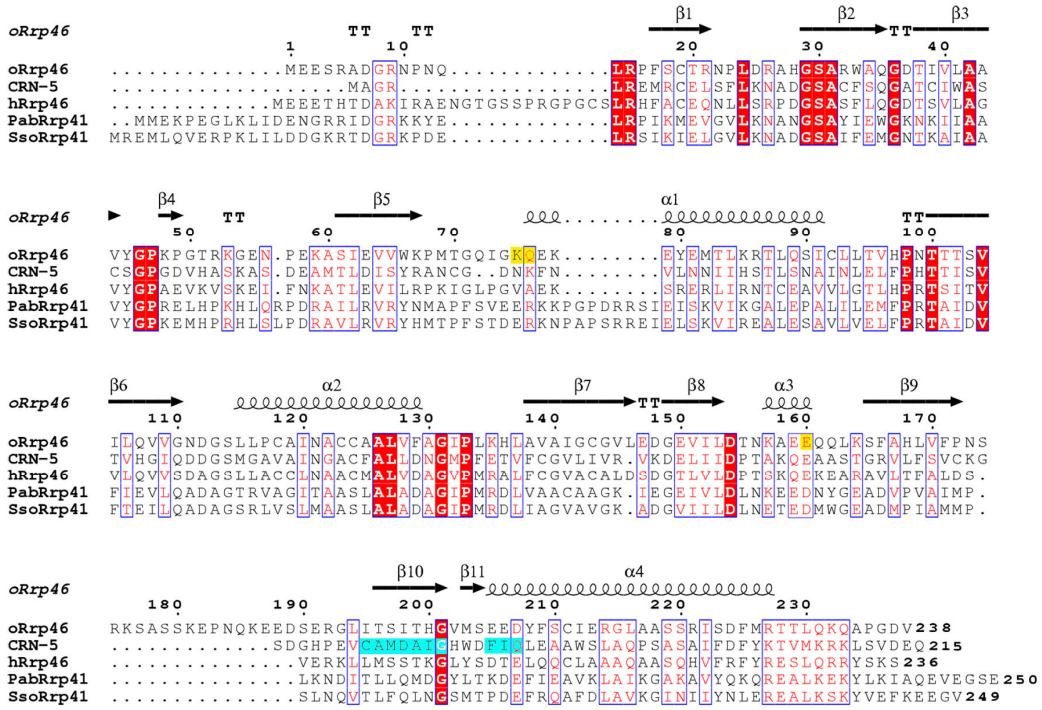

Figure 1-5. Sequence alignment of rice, human, and *C. elegans* Rrp46 (CRN-5) and archaeal Rrp41.

Eukaryotic Rrp46 shares significant sequence identity with archaeal Rrp41. Sequences listed here are Rrp46 from *Oryza sativa* (oRrp46), *Caenorhabditis elegans* (CRN-5), and human (hRrp46); and Rrp41 from *Pyrococcus abyssi* (PabRrp41) and *Sulfolobus solfataricus* (SsoRrp41). The secondary structure generated from the crystal structure of oRrp46 is shown above the sequence. TT represents β-turns. Identical and similar residues are colored in red. Mutational residues constructed in this study are colored in yellow. The residues involved in homo-dimeric interactions in CRN-5 are colored in cyan. The alignment was generated by ClustalW (http://www.ch.embnet.org/software/ClustalW.html) and ESpript (Gouet et al., 2003).

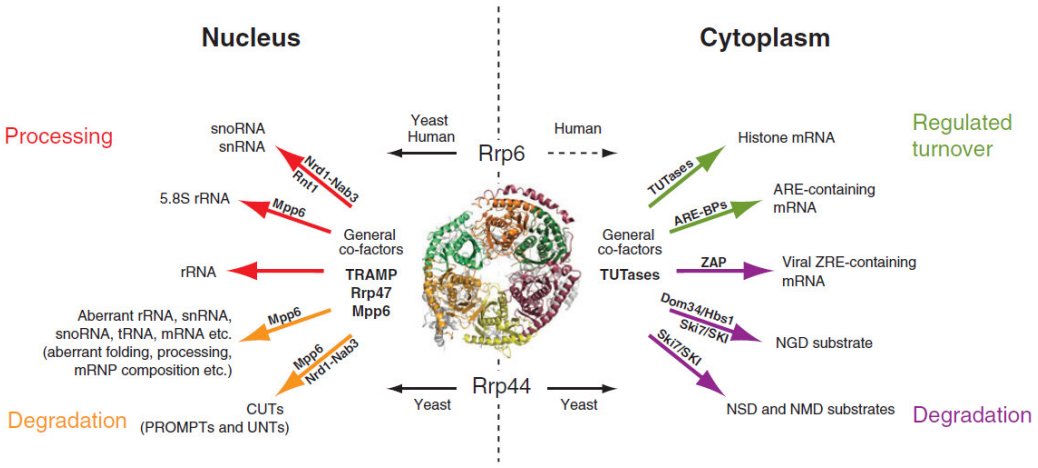

Figure 1-6. Diverse functions of the eukaryotic exosome (Lykke-Andersen et al., 2009)**.**

The nuclear and cytoplasmic processes maintained by the eukaryotic exosome are listed on the left and right, respectively. The active nucleases Rrp6 and Rrp44 are indicated above and below the core exosome. Arrows point to the subcellular compartments in which the nucleases have been shown to localise. Also indicated are the organism(s) in which this localisation has been determined. The dashed arrow pointing to the cytoplasm for human Rrp6 indicates that this localisation pattern is still disputed. The compartmentalised processes are further subdivided into pathways of nuclear RNA processing (red arrows) and degradation (orange arrows) on one side, and regulated cytoplasmic RNA turnover (green arrows) and degradation (purple arrows) on the other. Co-factors that are directly linked to the action of the exosome on specific RNA substrates are indicated above and below the arrows (although other pathway-specific factors might be involved in each case). Putative general nuclear and cytoplasmic co-factors are indicated immediately to the left and right of the exosome, respectively.

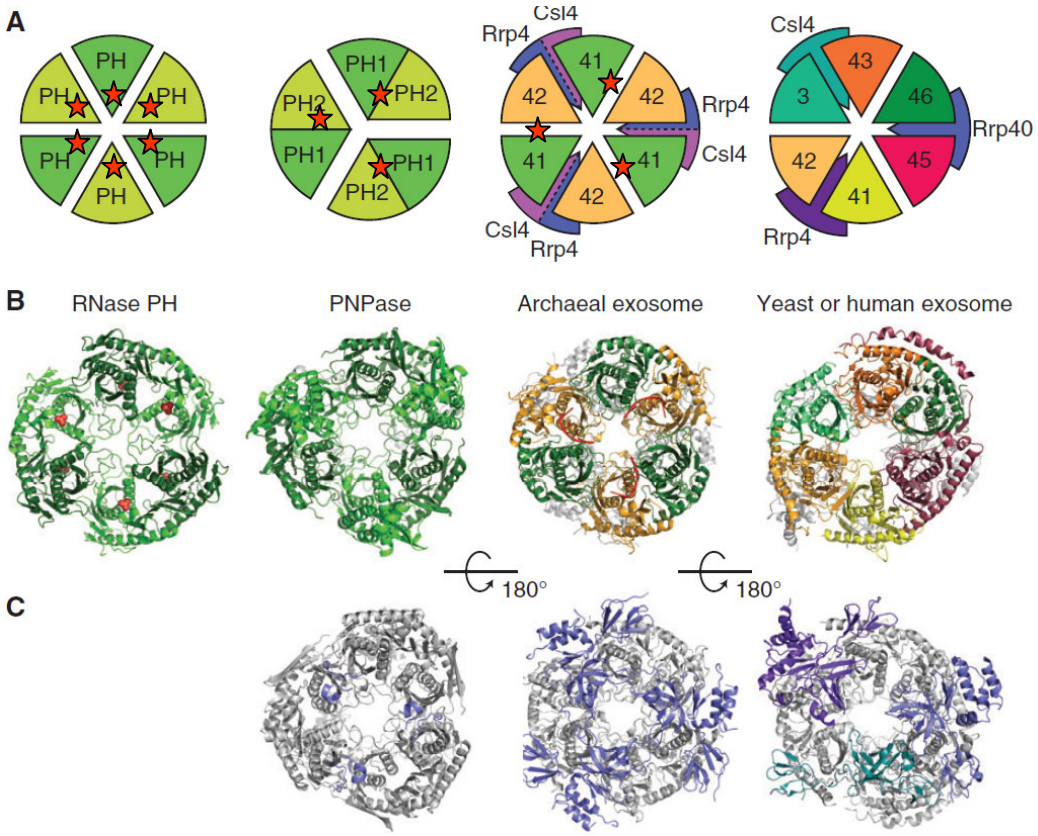

Figure 1-7. Architectures and structures of RNase PH, PNPase and exosome complex (Lykke-Andersen et al., 2009)**.**

(A) Schematic diagrams illustrate the subunit composition and orientation in bacterial RNase PH (dark green and light green show the inversely oriented arrangement of neighbouring subunits), bacterial PNPase (combined wedges illustrate PH domains from the same polypeptide chain), the archaeal exosome complex and the *S. cerevisiae* and human exosome complex. The diagrams show the complexes from 'underneath', with the RNA-binding cap of the archaeal exosome and *S. cerevisiae* and human exosome shown as extra wedges behind (blue and purple). In the case of the archaeal exosome, the two-tone wedges indicate that the three RNA-binding proteins in each complex can be either Rrp4, Csl4 or a combination of these. Active sites were indicated in red stars. (B) Actual structures of complexes shown in the same orientation, with domains in similar colours to those in (A). The structures shown are PDB 1UDN [RNase PH (Ishii et al., 2003)], 1E3H [PNPase (Symmons et al., 2000)], 2JEA [archaeal

exosome (Lorentzen et al., 2007)] and 2NN6 [human exosome (Liu et al., 2006)]. The RNA- binding caps are displayed in the background coloured in grey. Active sites are illustrated by the red colouration of the inorganic phosphate (for RNase PH) or RNA substrate (for the archaeal exosome). (C) Anterior views of PNPase, the archaeal exosome and the *S. cerevisiae* and human exosomes, with RNA-binding cap proteins shown in blue, purple and cyan.

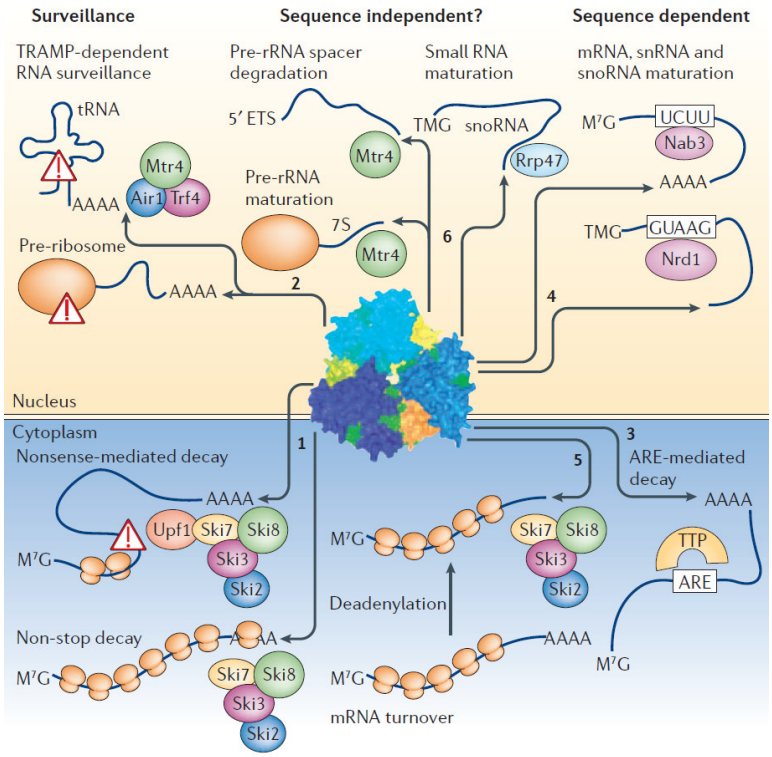

Figure 1-8. Activation of the eukaryotic exosome (Houseley et al., 2006)**.**

Despite the presence of several catalytic sites, the exosome is almost entirely inactive without the aid of cofactors. A diverse array of substrates and activating cofactors have been identified, and they fit broadly into four categories: surveillance, sequence-dependent degradation, sequence-independent degradation and maturation. **1**. The cytoplasmic exosome is activated by the Ski complex (Ski2–Ski3–Ski8), along with the helicase Ski7, for the degradation of improperly processed RNAs such as those lacking a stop codon (non-stop decay) or containing a premature stop codon (nonsense-mediated decay (NMD)). **2.** In the nucleus, the TRAMP complex (Trf4–Air1–Mtr4 in the diagram) targets defective precursors to ribosomal RNAs , transfer RNAs , small nuclear RNAs (snRNAs), small nucleolar RNAs (snoRNAs) and other transcripts. **3.** Sequence-dependent recruitment of the cytoplasmic exosome in human cells involves factors including TTP and KSRP (not shown), which directly recognize A+U-rich sequence elements (AREs) and cause mRNA destabilization.

4. In the nucleus, Nrd1, perhaps acting together with its binding partner Nab3, can recruit the exosome to mRNAs, snoRNAs and probably other RNAs that contain defined sequence motifs. Other exosome substrates lack defined sequence motifs that could specifically function in exosome recruitment. **5.** All mRNAs undergo turnover, a process that is not generally dependent on defined RNA sequences but that involves the Ski complex and the exosome, as well as the decapping and 5′-degradation machinery. **6.** In the nucleus, exosome-dependent RNA-degradation pathways that are unlikely to involve the recognition of simple RNA sequences include the degradation of spacer elements that have been excised from rRNA precursors and the 3′trimming of pre-rRNAs and snoRNAs. However, these activities require cofactors: the RNA helicase Mtr4 or the putative RNA-binding protein Rrp47. 7S is a 3′-extended precursor to the 5.8S rRNA, which is 3′matured by the exosome. ETS, external transcribed spacer; M7G, 7-methylguanosine; TMG, trimethylguanosine.

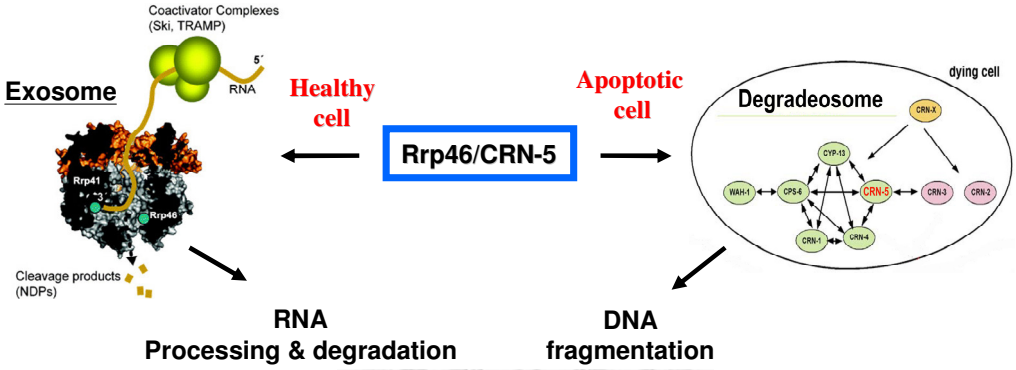

Figure 1-9.The hypothesis of dual fucntions of Rrp46/CRN-5 in healthy and apoptotic cells.

Rrp46/CRN-5 associates with exosome and is involved in RNA processing and degradation in living cells. During apoptosis, it switches its role to a DNase, and participates in apoptotic DNA degradation

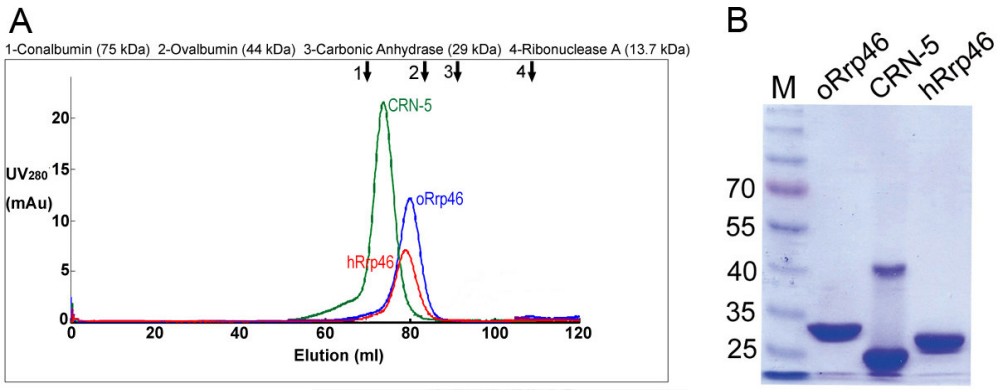

Figure 3-1. Gel filtration and SDS-PAGE analysis of purified Rrp46/CRN-5 proteins.

(A) Gel filtration (Superdex 200) profiles for hRrp46, oRrp46 and CRN-5. The recombinant Rrp46/CRN-5 all eluted with a size of a homodimer in a buffer of 25 mM Tris-HCl (pH 7.6), 150 mM NaCl and 1 mM β-mercaptoethanol. (B) The purified recombinant Rrp46 proteins from different species were analyzed by SDS-PAGE. CRN-5 was less homogeneous with strong linked dimers that could not be dissociated into monomers on SDS-PAGE under the reduced condition. Molecular weight markers (kD) are shown as indicated.

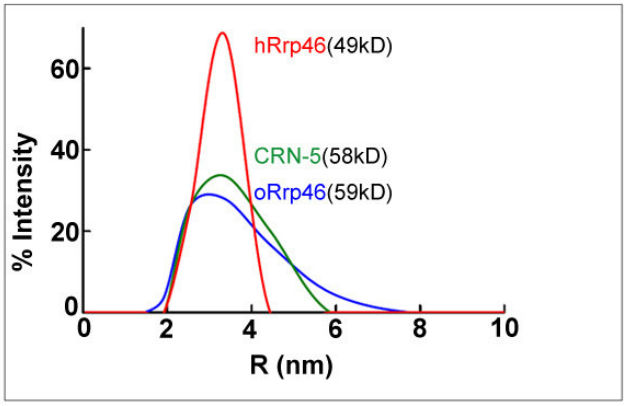

Figure 3-2. Dynamic light scattering (DLS) analysis of native Rrp46 proteins.

The estimated molecular weights of each protein (in parentheses) are listed in the figure.

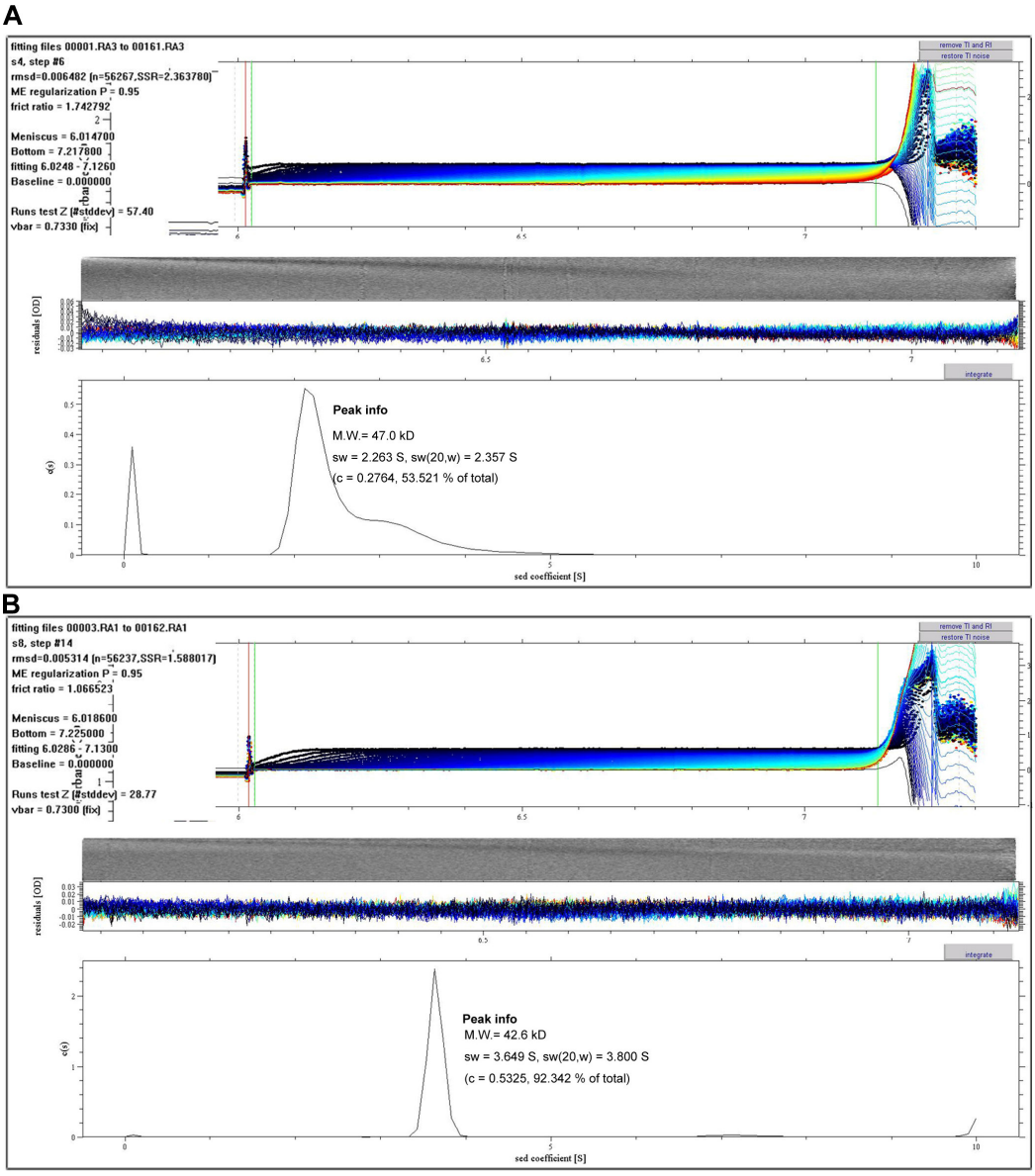

Figure 3-3. Sedimentation velocity analysis of human hRrp46 (A) and *C. elegans* CRN-5 (B) by analytical ultracentrifugation.

Upper: sedimentation velocity absorbance trace of the sample at 280 nm. Values used in data calculation and validation were shown at left. Middle: residuals of the experimental fits. Lower: continuous sedimentation coefficient distribution of the protein. The information after peak integration was shown at right of the peak.

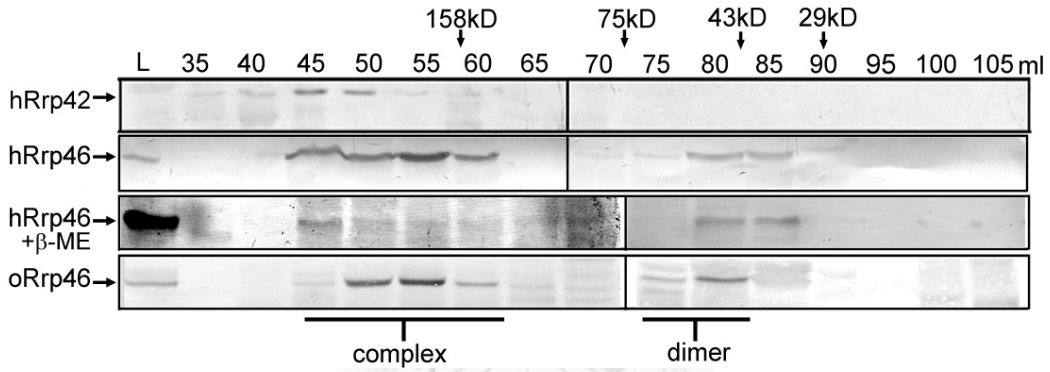

Figure 3-4. Endogenous Rrp46 proteins were detected by Western blotting after gel filtration fractionation of cell extracts.

Endogenous Rrp46 either formed homodimers, or associated with a protein complex. Human (293T) and rice (callus) cell extracts were fractionated on a Superdex 200 gel-filtration column in a buffer with (+β-ME) or without β-mercaptoethanol and analyzed by Western blotting using rabbit anti-hRrp42, anti-hRrp46 or anti-oRrp46 serum. The hRrp42 was used as a control to show that it only associated with a protein complex. The cell extract before fractionation is shown in lane L. Molecular weight markers are shown as indicated.

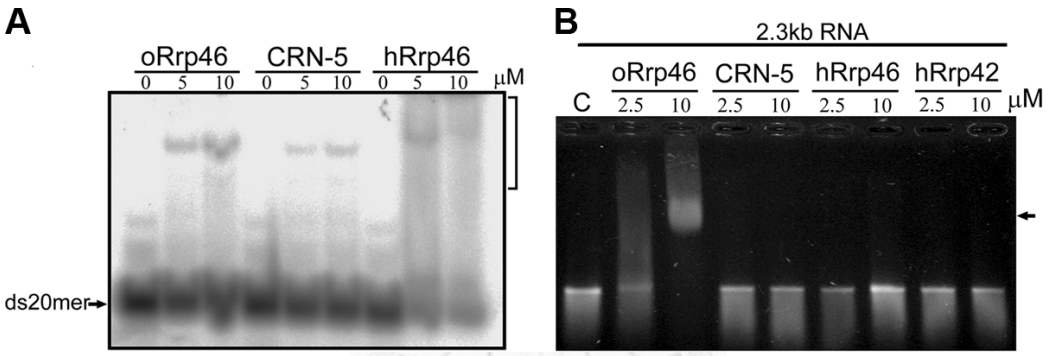

Figure 3-5. DNA- and RNA-binding assays of CRN-5 and Rrp46 proteins.

(A) Gel-retardation assays show that Rrp46 binds to double-stranded DNA. Rrp46 (0, 5 and 10 μM) were incubated with 20-mer DNA (20 nM) in the buffer of 20 mM HEPES (pH 7.0) and 5 mM EDTA. The protein-DNA complexes were indicated by a bracket marked at the right of the panel. (B) Gel retardation assays show that only rice oRrp46 binds to RNA. *In vitro* transcribed RNA (500 ng) was incubated with Rrp46 (2.5 or 10 μM) in the RNA-binding buffer (50 mM Tris, pH 8.0, 10 mM EDTA, 1 U/μl RNaseIN) on ice for 30 minutes. The up-shifted RNA was indicated by an arrow.

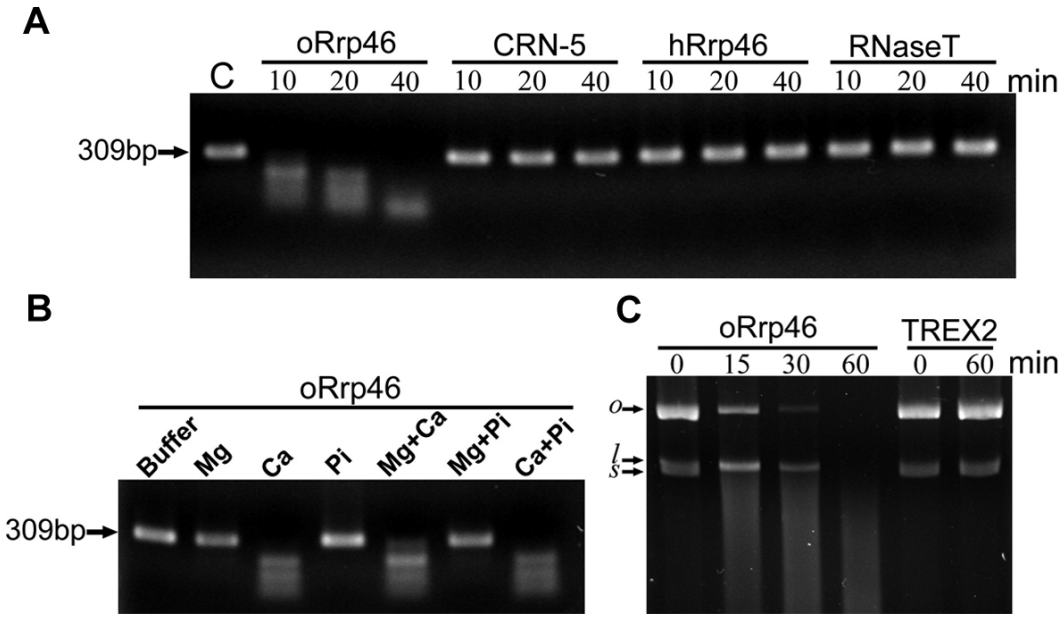

Figure 3-6. DNase activity assays of CRN-5 and Rrp46.

(A) DNA cleavage assays show that only rice oRrp46 cleaved double-stranded linear DNA. Rrp46 (1 μM) was incubated with the linear dsDNA (30 nM) in the DNase reaction buffer (20 mM HEPES (pH 7.0), 100 mM NaCl, 1 mM $CaCl_2$ and 1 mM DTT) at 37°C for the indicated periods, followed by agarose gel electrophoresis. A control reaction without any Rrp46 added is shown in lane C. RNA-specific RNase T was used as a negative control. (B) Rice oRrp46 is a metal ion-dependant hydrolytic DNase. oRrp46 (1 μM) was incubated with linear dsDNA (30 nM) at 37°C for 20 minutes in the presence or absence of $MgCl_2$, $CaCl_2$ and NaH_2PO_4. All the reaction buffers contained 20 mM HEPES (pH 7.0), 100 mM NaCl, 1 mM DTT with addition of 2 mM $MgCl_2$ in the lane labeled **Mg**, 1 mM $CaCl_2$ in the lane labeled **Ca**, 5 mM NaH_2PO_4 in the lane labeled **Pi**, and combination of each 2 factors in the rest of the lanes. A control reaction without metal and phosphate ion added is shown in lane labeled **Buffer**. (C) Rice oRrp46 cleaves plasmid DNA. oRrp46 (0.2 μM) was incubated with 100 ng plasmid DNA at 37°C for up to 60 min in the DNase reaction buffer. TREX2, an exonucleolytic hydrolase, was used as a negative control. *o*: open circular. *l*: linear. *s*: super coiled.

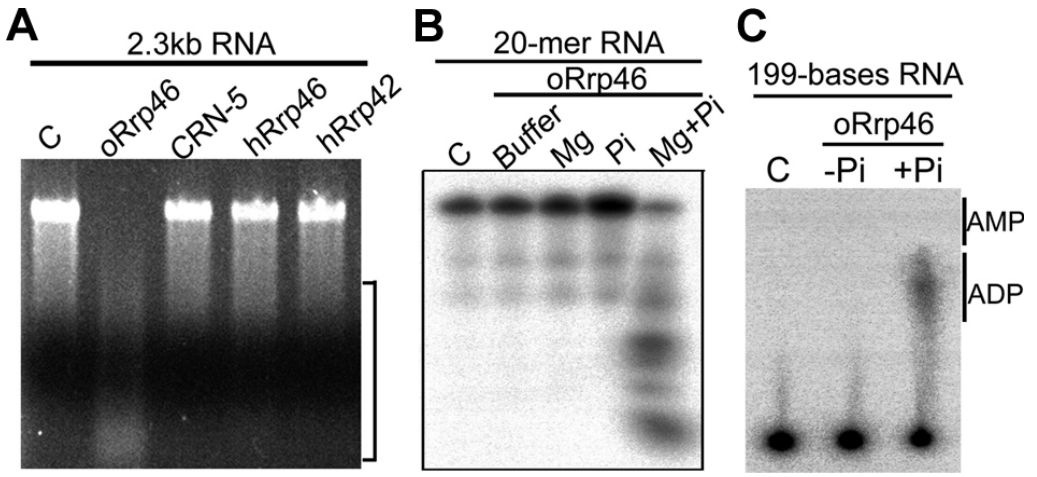

Figure 3-7. RNase activity assays of CRN-5 and Rrp46.

(A) RNA cleavage assays show that rice oRrp46 degrades RNA substrates. The bracket marked at the right indicates the degraded RNA. Rrp46 (5 μM) was incubated with the same substrate used in Fig. 4A in the RNase reaction buffer (50 mM Tris (pH 8.0), 50 mM KCl, 2 mM $MgCl_2$, 5 mM Na_2HPO_4 and 1U/μl RNaseIN) at 30^{o}C for 1 hour followed by agarose gel electrophoresis. (B) Rice oRrp46 is a metal ion- and phosphate-dependent RNase. oRrp46 (2 μM) was incubated with 5' labeled 20-mer ssRNA in conditions mentioned in Fig. 3C. A control reaction with both cofactors but without any Rrp46 added is shown in lane C. (C) Thin layer chromatography (TLC) separation of the final RNA reaction products cleaved by rice oRrp46. The internal ^{32}P-labeled RNA substrate was incubated with oRrp46 for 60 minutes with or without the presence of 5 mM phosphate (-Pi and +Pi). Positions of the cofractionated unlabeled ADP and AMP are shown on the right.

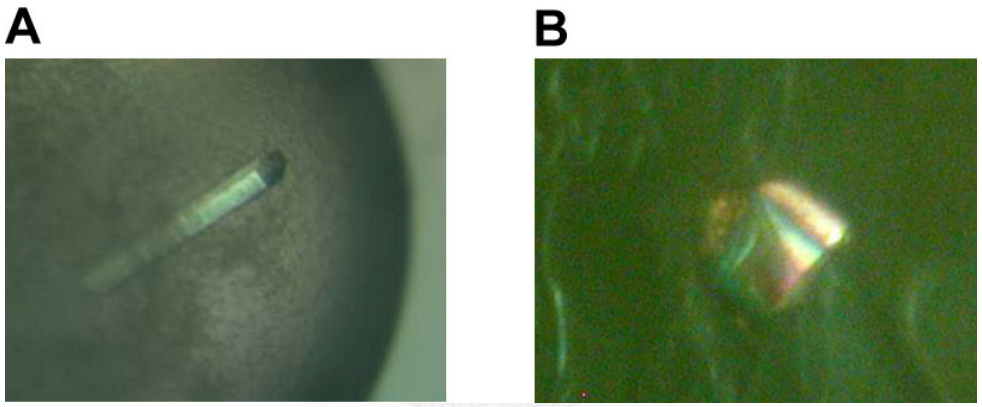

Figure 3-8. Crystals of rice oRrp46 and *C. elegans* CRN-5.

(A) A crystal of rice oRrp46. (B) A crystal of *C. elegans* CRN-5.

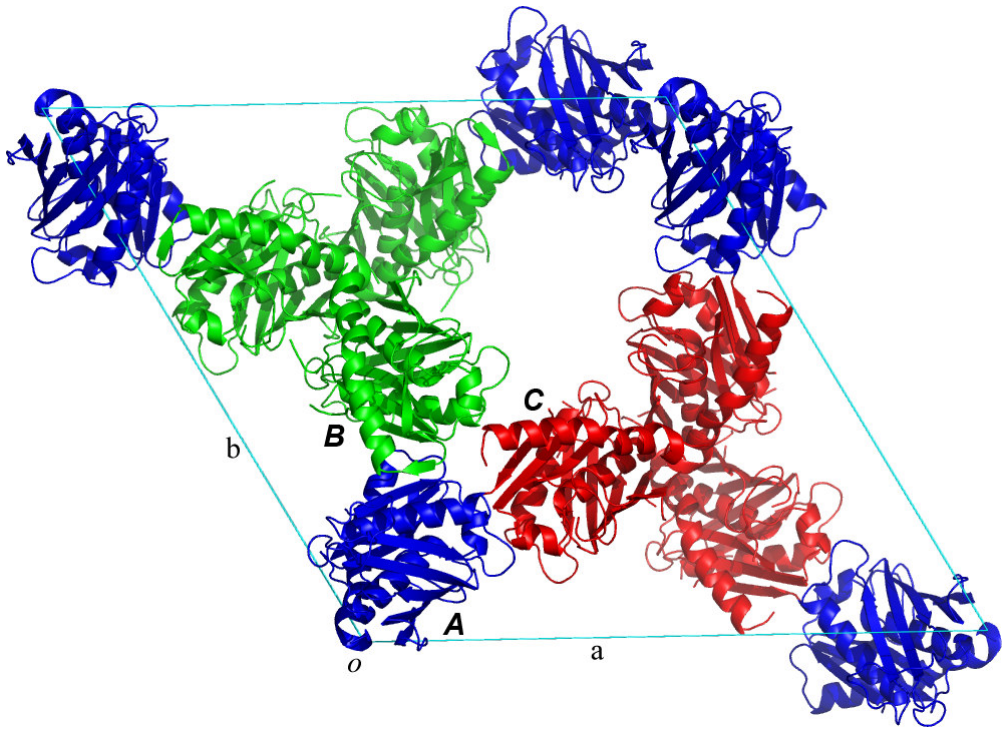

Figure 3-9. Crystal packing of rice oRrp46.

Crystal packing of rice oRrp46 in an unit cell (cyan line). There are 3 molecules in an asymmetric unit. They are molecule A in blue, molecule B in green and molecule C in red. o : origin. a : a axis. b : b axis.

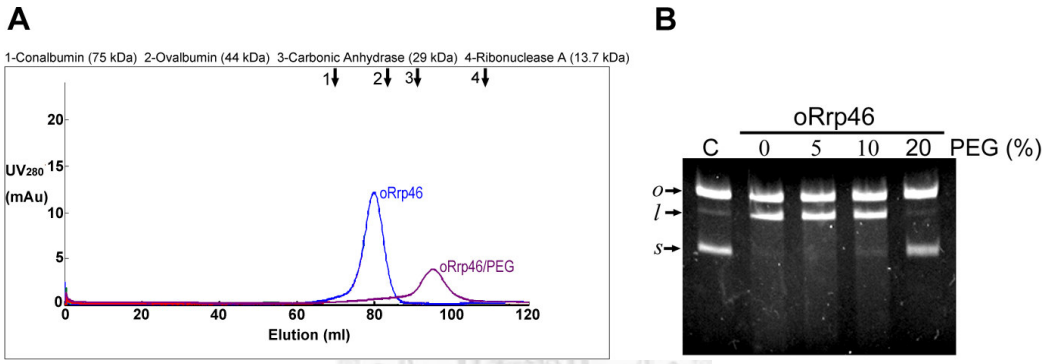

Figure 3-10. Rice oRrp46 dissociates into monomer and losts DNase activity by PEG.

(A) Gel filtration (Superdex 200) profiles for oRrp46 in the presence (purple) or absence (blue) of PEG3350. oRrp46 shifted into monomers with the addition of 5% PEG 3350 (oRrp46/PEG). (B) Rice oRrp46 lost its DNase activity in the presence of PEG3350. oRrp46 (0.2 μM) was incubated with 100 ng plasmid DNA at 37°C for 30 min in the presence of various concentration (0-20%) of PEG3350. Lane C is for loading control. *o*: open circular. *l*: linear. *s*: super coiled.

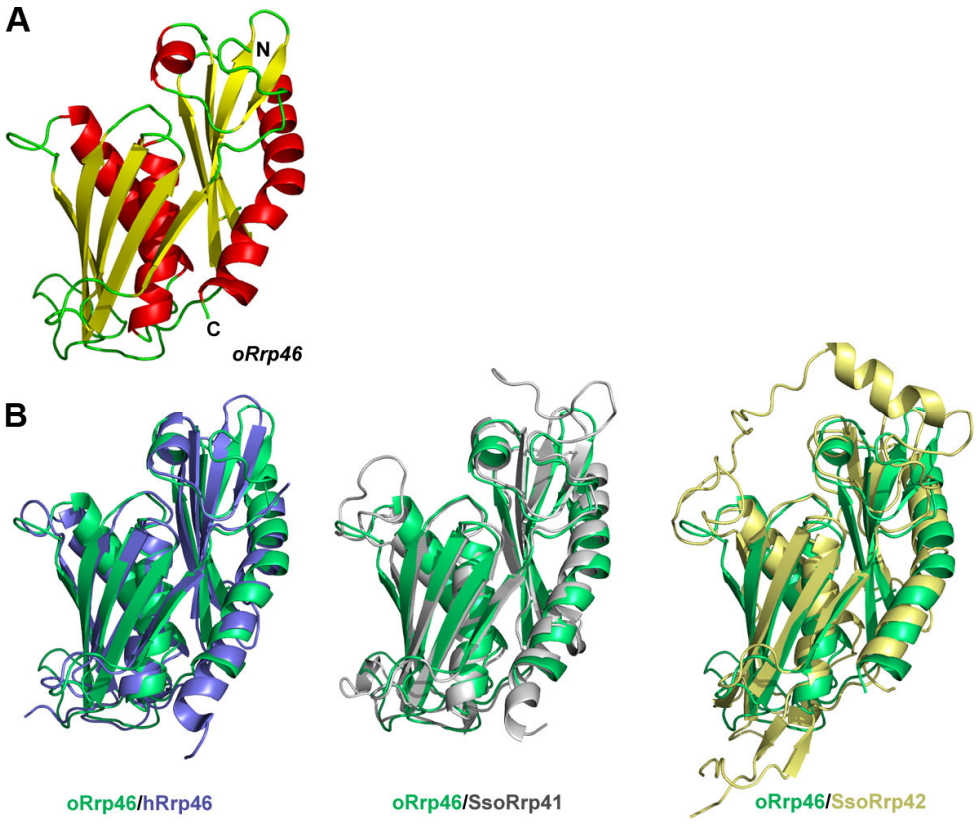

Figure 3-11. Crystal structure of the monomeric oRrp46.

(A) The crystal structure of the monomeric oRrp46. The color was presented according to secondary structure. α-helix : red. β-sheet : yellow. Turn : green. The N-terminal and C-terminal were shown in N and C, respectively. (B) Superposition of the crystal structure of rice oRrp46 onto human hRrp46 (2NN6, chain D. RMSD of 1.29 Å over 187 C_α atoms), archaeal Rrp41 (2JEA, chain B. RMSD of 1.32 Å over 202 C_α atoms) and archaeal Rrp42 (2JEA, chain A. RMSD of 1.49 Å over 197 C_α atoms).

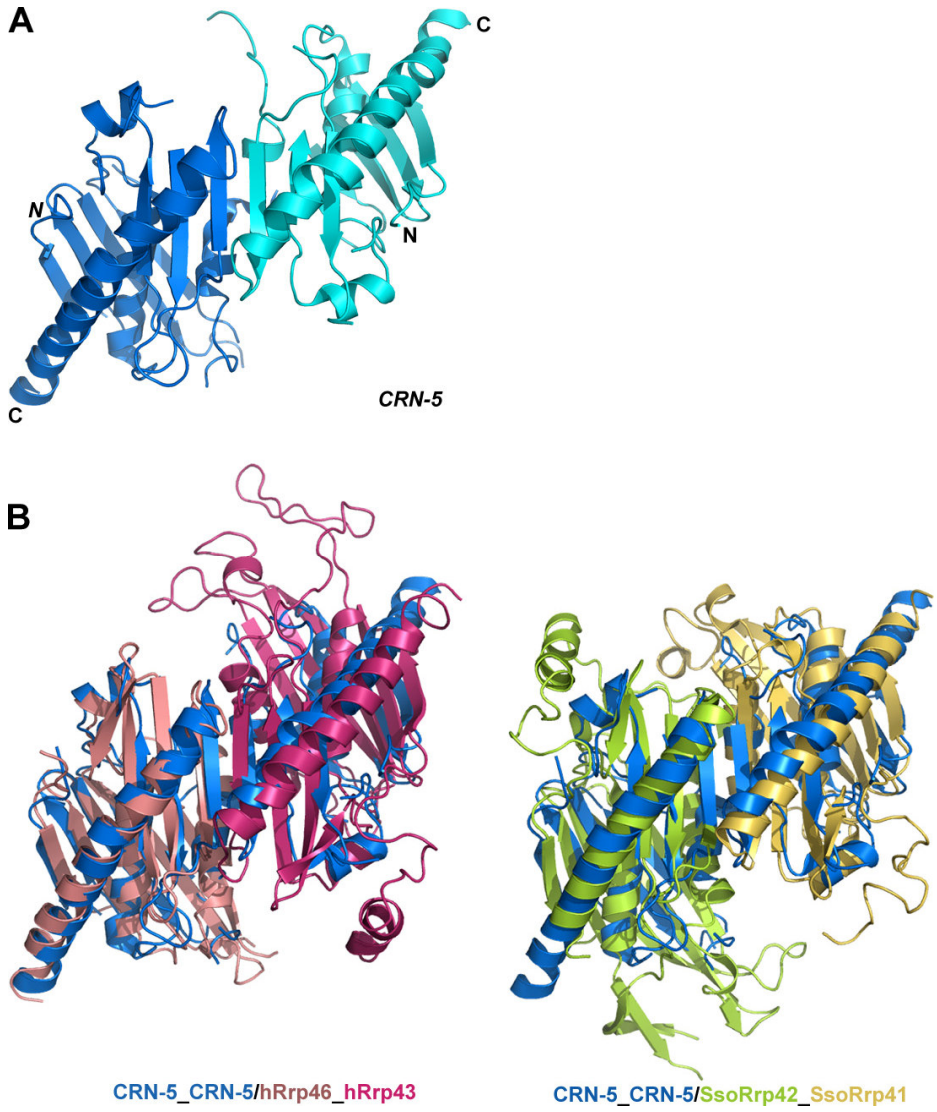

Figure 3-12. Crystal structure of the dimeric CRN-5.

(A) The crystal structure of the dimeric CRN-5. Individual monomers are shown in blue and cyan, respectively. (B) Superposition of the crystal structure of homodimeric CRN-5 onto human hRrp46_hRrp43 heterodimer (RMSD of 3.05 Å over 273 C_α atoms) and archaeal Rrp41_Rrp42 heterodimer (RMSD of 3.02 Å over 279 C_α atoms).

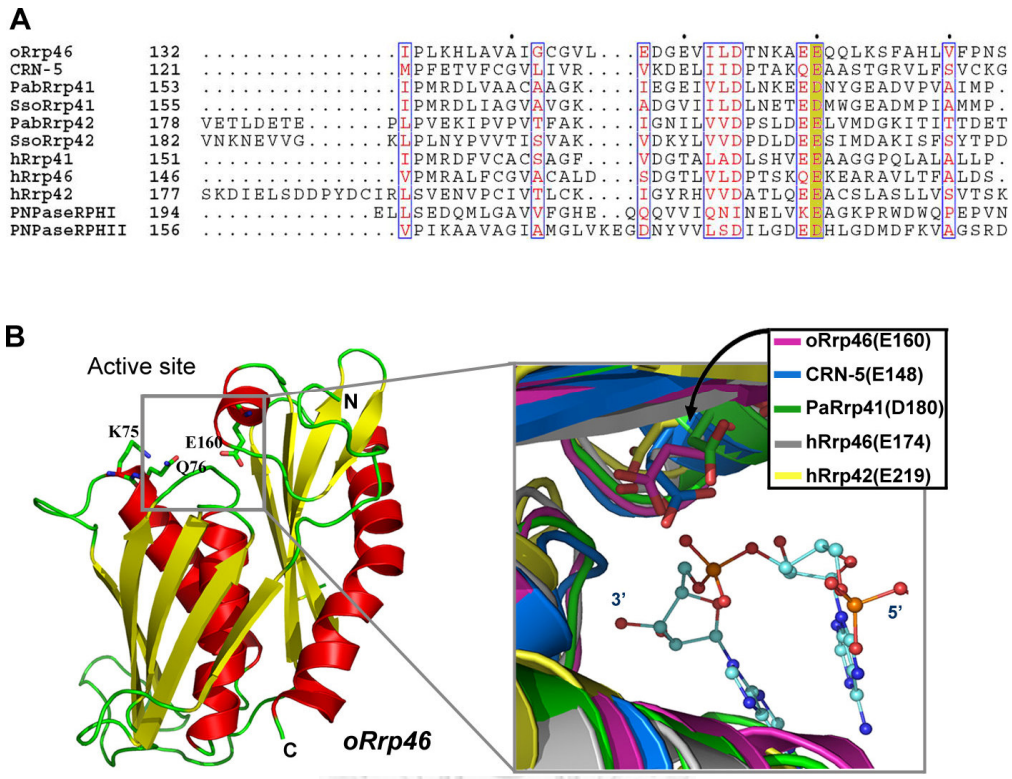

Figure 3-13. A metal binding residue is conserved in RNase PH family protein.

(A) Sequence alignments of RNase PH proteins from various species. This conserved metal-binding residue (colored in yellow) is conserved in both active and inactive RNase PH proteins. PabRrp41 and PabRrp42 are from *Pyrococcus abyssi*. SsoRrp41 and SsoRrp42 are from *Sulfolobus solfataricus*. PNPase is from *E. coli*. (B) Superposition of the active sites of several RNase PH proteins shows that a conserved acidic residue is located at the same position: E160 in oRrp46 (this study), E148 in CRN-5 (this study), D180 in PaRrp42 (2PO1, chain A), E174 in hRrp46 (2NN6, chain D) and E219 in hRrp42 (2NN6, chain E). The bound RNA nucleotide co-crystallized with PaRrp41 is displayed as a ball-and-stick model.

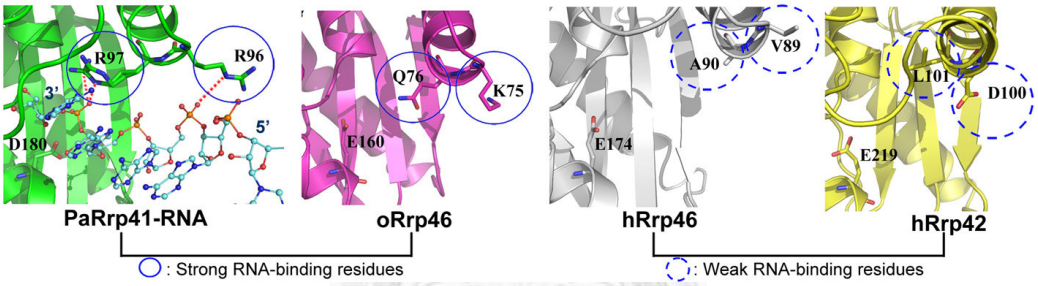

Figure 3-14. Comparison of RNA-binding residues in RNase PH proteins.

The two basic residues, R96 and R97, bind to the phosphate groups of RNA (displayed as a ball-and-stick model) in PaRrp41 (green, 2PO1, chain A). Corresponding residues in oRrp46 (Q76 and K75) are more suitable for RNA binding compared to those in the inactive enzymes of hRrp46 (V89 and A90) and hRrp42 (D100 and L101). The strong RNA-binding residues are circled in solid lines and the weak RNA-binding residues are circled in dashed lines.

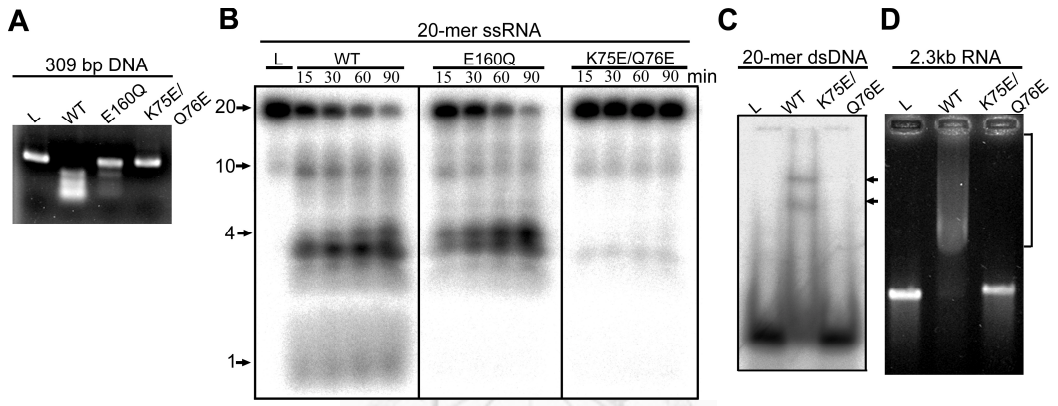

Figure 3-15. *In vitro* nuclease activity assays of wild-type and mutated oRrp46.

(A) DNA (309 bp, 30 nM) cleavage assays by the wild type, active-site mutant (E160Q), and nucleotide-binding-site mutant (K75E/Q76E) of oRrp46 (1 μM). All the reaction conditions were identical to those in Fig. 3-5 to 3-7. (B) Time-course RNA cleavage assays by the wild type, E160Q and K75E/Q76E mutant of oRrp46. The RNA markers varied from 1-20 nucleotide(s) were labeled at the left of the panel. (C) DNA gel shift assays of wild type and K75E/Q76E mutant of oRrp46. The protein-DNA complex was indicated by an arrow. (D) RNA gel shift assays of wild type and K75E/Q76E mutant of oRrp46. The up-shifted RNA was indicated by an arrow. The bracket marked at the right indicates the up-shifted RNA.

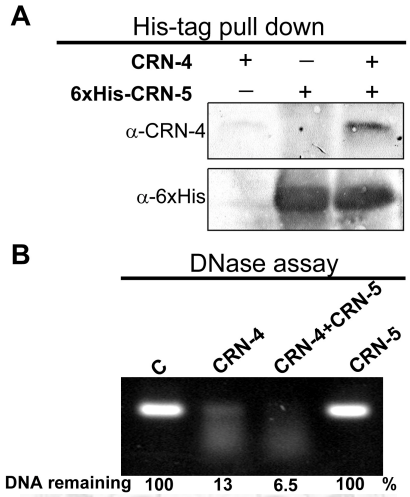

Figure 3-16. CRN-5 interacts with CRN-4 and enhances CRN-4's DNase activity. (A) His-tag pull down assays of CRN-4 by His-tagged CRN-5. The His-tagged CRN-5 was incubated with or without CRN-4, and then the complex was pulled down in a Ni-NTA spin column. The eluted solution was analyzed by Western blotting using anti-CRN-4 (α-CRN-4) and anti-6xHis (α-6xHIS) antibodies. (B) Assays of CRN-4 DNase activity in the presence or absence of CRN-5. A linear 309-bp double-stranded DNA (30 nM) was incubated with CRN-4 (1 μM), CRN-5 (2 μM), or both together, and the DNA digests were analyzed and quantified by gel electrophoresis. CRN-4 cleaved linear dsDNA more efficiently in the presence of inactive CRN-5 (6.5% vs. 13% DNA remained).

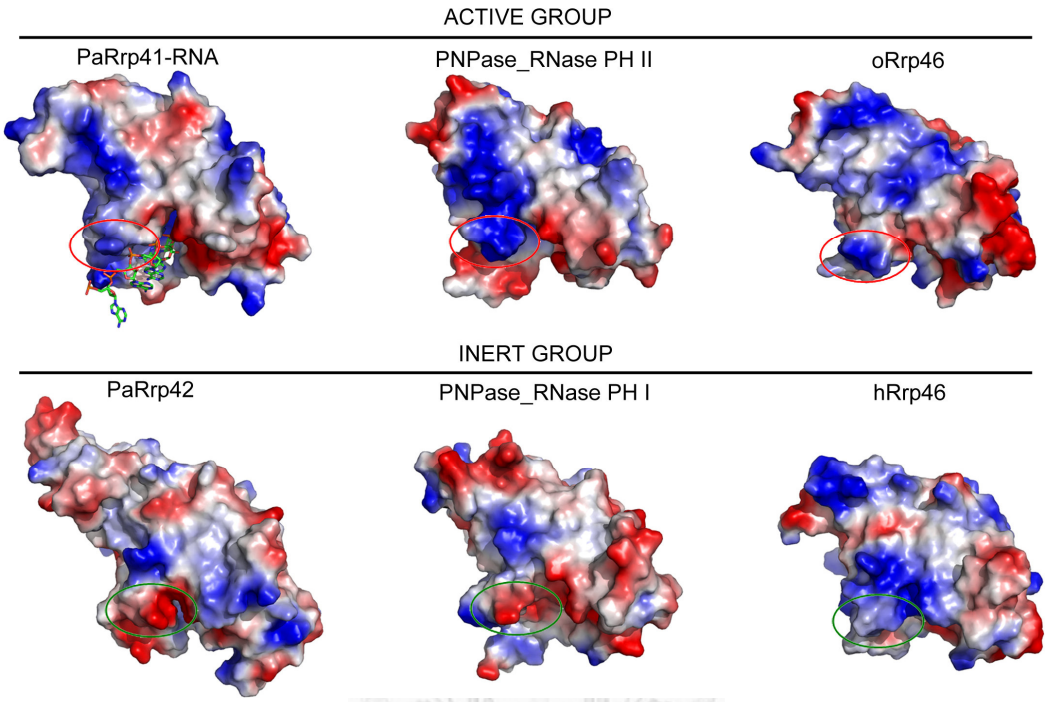

Figure 3-17. Electrostatic surface potential and substrate-binding sites of active and inactive RNase PH proteins.

The active RNase PH proteins all have positive surfaces at the RNA-binding site (circled), including PaRrp41 (2PO1, chain A), RNase PH II domain of PNPase (3CDI) and oRrp46 (this study). The RNA bound in PaRrp41 is displayed as a stick model. On the contrary, the inactive RNase PH proteins have neutral or acidic surfaces at the RNA-binding sites (circled), including PaRp42 (2PO1, chain B), RNase PH I domain of PNPase (3CDI) and hRrp46. The color scale of the surface potential was set from -75 kT/e (red) to 75 kT/e (blue), as calculated by Pymol (DeLano Scientific LLC, http://www.pymol.org).

A

Tissue	EST Data		
	Normal	Cancer	P
eye	6 / 130703	11 / 46531	0.003
lung	6 / 129126	21 / 172986	0.025
placenta	6 / 242058	6 / 39556	0.014
skin	0 / 74240	10 / 125548	0.027

B

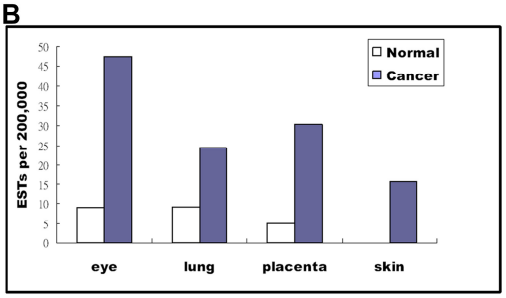

Figure 3-18. hRrp46 gene is upregulated in various cancer tissues.

(A) Comparison of human hRrp46 expressed sequence tag (EST) in normal and cancer tissues. Cancer Genome Anatomy Project (CGAP; http://cgap.nci.nih.gov) data was mined for the EST number of hRrp46 or other exosomal component (data not shown) genes in normal and cancer tissues. hRrp46's EST number out of total EST database was shown in columns. The appearance pattern of hRrp46 EST in cancer (eye, lung, placenta and skin) and normal tissues is with statistical differences ($P<0.05$). (B) Expression level of hRrp46 gene in normal and cancer tissues. The original appearance EST number of hRrp46 out of total EST database in (A) was converted into appearance frequency in ever 200,000 tags. hRrp46 gene is highly expressed in cancer tissues more than 2 fold to that in normal tissues.

REFERENCES

Adams, P.D., Grosse-Kunstleve, R.W., Hung, L.W., Ioerger, T.R., McCoy, A.J., Moriarty, N.W., Read, R.J., Sacchettini, J.C., Sauter, N.K., and Terwilliger, T.C. (2002). PHENIX: building new software for automated crystallographic structure determination. Acta Crystallogr D Biol Crystallogr *58*, 1948-1954.

Alderuccio, F., Chan, E.K., and Tan, E.M. (1991). Molecular characterization of an autoantigen of PM-Scl in the polymyositis/scleroderma overlap syndrome: a unique and complete human cDNA encoding an apparent 75-kD acidic protein of the nucleolar complex. J Exp Med *173*, 941-952.

Allmang, C., Kufel, J., Chanfreau, G., Mitchell, P., Petfalski, E., and Tollervey, D. (1999a). Functions of the exosome in rRNA, snoRNA and snRNA synthesis. EMBO J *18*, 5399-5410.

Allmang, C., Mitchell, P., Petfalski, E., and Tollervey, D. (2000). Degradation of ribosomal RNA precursors by the exosome. Nucleic Acids Res *28*, 1684-1691.

Allmang, C., Petfalski, E., Podtelejnikov, A., Mann, M., Tollervey, D., and Mitchell, P. (1999b). The yeast exosome and human PM-Scl are related complexes of 3' --> 5' exonucleases. Genes Dev *13*, 2148-2158.

Anderson, J.S., and Parker, R.P. (1998). The 3' to 5' degradation of yeast mRNAs is a general mechanism for mRNA turnover that requires the SKI2 DEVH box protein and 3' to 5' exonucleases of the exosome complex. EMBO J *17*, 1497-1506.

Andreeva, L., Heads, R., and Green, C.J. (1999). Cyclophilins and their possible role in the stress response. International Journal of Experimental Pathology *80*, 305-315.

Andrulis, E.D., Werner, J., Nazarian, A., Erdjument-Bromage, H., Tempst, P., and Lis, J.T. (2002). The RNA processing exosome is linked to elongating RNA polymerase II in Drosophila. Nature *420*, 837-841.

Araki, Y., Takahashi, S., Kobayashi, T., Kajiho, H., Hoshino, S., and Katada, T. (2001). Ski7p G protein interacts with the exosome and the Ski complex for 3'-to-5' mRNA decay in yeast. EMBO J *20*, 4684-4693.

Arigo, J.T., Carroll, K.L., Ames, J.M., and Corden, J.L. (2006a). Regulation of yeast NRD1 expression by premature transcription termination. Mol Cell *21*, 641-651.

Arigo, J.T., Eyler, D.E., Carroll, K.L., and Corden, J.L. (2006b). Termination of cryptic unstable transcripts is directed by yeast RNA-binding proteins Nrd1 and Nab3. Mol Cell *23*, 841-851.

Baginsky, S., Shteiman-Kotler, A., Liveanu, V., Yehudai-Resheff, S., Bellaoui, M., Settlage, R.E., Shabanowitz, J., Hunt, D.F., Schuster, G., and Gruissem, W. (2001). Chloroplast PNPase exists as a homo-multimer enzyme complex that is distinct from the Escherichia coli degradosome. RNA *7*, 1464-1475.

Bluthner, M., and Bautz, F.A. (1992). Cloning and characterization of the cDNA coding for a polymyositis-scleroderma overlap syndrome-related nucleolar 100-kD protein. J Exp Med *176*, 973-980.

Bonneau, F., Basquin, J., Ebert, J., Lorentzen, E., and Conti, E. (2009). The yeast exosome functions as a macromolecular cage to channel RNA substrates for degradation. Cell *139*, 547-559.

Bousquet-Antonelli, C., Presutti, C., and Tollervey, D. (2000). Identification of a regulated pathway for nuclear pre-mRNA turnover. Cell *102*, 765-775.

Briggs, M.W., Burkard, K.T., and Butler, J.S. (1998). Rrp6p, the yeast homologue of the human PM-Scl 100-kDa autoantigen, is essential for efficient 5.8 S rRNA 3' end formation. J Biol Chem *273*, 13255-13263.

Brouwer, R., Pruijn, G.J., and van Venrooij, W.J. (2001). The human exosome: an autoantigenic complex of exoribonucleases in myositis and scleroderma. Arthritis Res *3*, 102-106.

Brouwer, R., Vree Egberts, W.T., Hengstman, G.J., Raijmakers, R., van Engelen, B.G., Seelig, H.P., Renz, M., Mierau, R., Genth, E., Pruijn, G.J.*, et al.* (2002). Autoantibodies directed to novel components of the PM/Scl complex, the human exosome. Arthritis Res *4*, 134-138.

Brown, J.T., Bai, X., and Johnson, A.W. (2000). The yeast antiviral proteins Ski2p, Ski3p, and Ski8p exist as a complex in vivo. RNA *6*, 449-457.

Brown, P.H., and Schuck, P. (2006). Macromolecular size-and-shape distributions by sedimentation velocity analytical ultracentrifugation. Biophys J *90*, 4651-4661.

Burkard, K.T., and Butler, J.S. (2000). A nuclear 3'-5' exonuclease involved in mRNA degradation interacts with Poly(A) polymerase and the hnRNA protein Npl3p. Mol Cell Biol *20*, 604-616.

Buttner, K., Wenig, K., and Hopfner, K.P. (2005). Structural framework for the mechanism of archaeal exosomes in RNA processing. Mol Cell *20*, 461-471.

Buttner, S., Eisenberg, T., Carmona-Gutierrez, D., Ruli, D., Knauer, H., Ruckenstuhl, C., Sigrist, C., Wissing, S., Kollroser, M., Frohlich, K.U.*, et al.* (2007). Endonuclease G regulates budding yeast life and death. Mol Cell *25*, 233-246.

Chekanova, J.A., Shaw, R.J., Wills, M.A., and Belostotsky, D.A. (2000). Poly(A) tail-dependent exonuclease AtRrp41p from *Arabidopsis thaliana* rescues 5.8 S rRNA processing and mRNA decay defects of the yeast ski6 mutant and is found in an exosome-sized complex in plant and yeast cells. J Biol Chem *275*, 33158-33166.

Chen, C.Y., Gherzi, R., Ong, S.E., Chan, E.L., Raijmakers, R., Pruijn, G.J., Stoecklin, G., Moroni, C., Mann, M., and Karin, M. (2001). AU binding proteins recruit the exosome to degrade ARE-containing mRNAs. Cell *107*, 451-464.

Collins, R.H., Jr., Shpilberg, O., Drobyski, W.R., Porter, D.L., Giralt, S., Champlin, R.,

Goodman, S.A., Wolff, S.N., Hu, W., Verfaillie, C., *et al.* (1997). Donor leukocyte infusions in 140 patients with relapsed malignancy after allogeneic bone marrow transplantation. J Clin Oncol *15*, 433-444.

de la Cruz, J., Kressler, D., Tollervey, D., and Linder, P. (1998). Dob1p (Mtr4p) is a putative ATP-dependent RNA helicase required for the 3' end formation of 5.8S rRNA in Saccharomyces cerevisiae. EMBO J *17*, 1128-1140.

Deutscher, M.P., Marshall, G.T., and Cudny, H. (1988). RNase PH: an Escherichia coli phosphate-dependent nuclease distinct from polynucleotide phosphorylase. Proc Natl Acad Sci U S A *85*, 4710-4714.

Doma, M.K., and Parker, R. (2006). Endonucleolytic cleavage of eukaryotic mRNAs with stalls in translation elongation. Nature *440*, 561-564.

Dominski, Z., Yang, X.C., Kaygun, H., Dadlez, M., and Marzluff, W.F. (2003). A 3' exonuclease that specifically interacts with the 3' end of histone mRNA. Mol Cell *12*, 295-305.

Duchaine, T.F., Wohlschlegel, J.A., Kennedy, S., Bei, Y., Conte, D., Jr., Pang, K., Brownell, D.R., Harding, S., Mitani, S., Ruvkun, G., *et al.* (2006). Functional proteomics reveals the biochemical niche of C. elegans DCR-1 in multiple small-RNA-mediated pathways. Cell *124*, 343-354.

Durrieu, F., Samejima, K., Fortune, J.M., Kandels-Lewis, S., Osheroff, N., and Earnshaw, W.C. (2000). DNA topoisomerase IIalpha interacts with CAD nuclease and is involved in chromatin condensation during apoptotic execution. Curr Biol *10*, 923-926.

Dziembowski, A., Lorentzen, E., Conti, E., and Seraphin, B. (2007). A single subunit, Dis3, is essentially responsible for yeast exosome core activity. Nat Struct Mol Biol *14*, 15-22.

Elbashir, S.M., Lendeckel, W., and Tuschl, T. (2001). RNA interference is mediated by 21- and 22-nucleotide RNAs. Genes Dev *15*, 188-200.

Emsley, P., and Cowtan, K. (2004). Coot: model-building tools for molecular graphics. Acta Crystallogr D Biol Crystallogr *60*, 2126-2132.

Enari, M., Sakahira, H., Yokoyama, H., Okawa, K., Iwamatsu, A., and Nagata, S. (1998). A caspase-activated DNase that degrades DNA during apoptosis, and its inhibitor ICAD. Nature *391*, 43-50.

Estevez, A.M., Kempf, T., and Clayton, C. (2001). The exosome of *Trypanosoma brucei*. EMBO J *20*, 3831-3839.

Evguenieva-Hackenberg, E., Walter, P., Hochleitner, E., Lottspeich, F., and Klug, G. (2003). An exosome-like complex in Sulfolobus solfataricus. EMBO Rep *4*, 889-893.

Ge, Q., Frank, M.B., O'Brien, C., and Targoff, I.N. (1992). Cloning of a complementary DNA coding for the 100-kD antigenic protein of the PM-Scl autoantigen. J Clin Invest

90, 559-570.

Gherzi, R., Lee, K.Y., Briata, P., Wegmuller, D., Moroni, C., Karin, M., and Chen, C.Y. (2004). A KH domain RNA binding protein, KSRP, promotes ARE-directed mRNA turnover by recruiting the degradation machinery. Mol Cell *14*, 571-583.

Gouet, P., Robert, X., and Courcelle, E. (2003). ESPript/ENDscript: Extracting and rendering sequence and 3D information from atomic structures of proteins. Nucleic Acids Res *31*, 3320-3323.

Green, D.R., Ferguson, T., Zitvogel, L., and Kroemer, G. (2009). Immunogenic and tolerogenic cell death. Nature Review Immun *9*, 353-363.

Guo, X., Ma, J., Sun, J., and Gao, G. (2007). The zinc-finger antiviral protein recruits the RNA processing exosome to degrade the target mRNA. Proceedings of the National Academy of Sciences *104*, 151-156.

Halenbeck, R., MacDonald, H., Roulston, A., Chen, T.T., Conroy, L., and Williams, L.T. (1998). CPAN, a human nuclease regulated by the caspase-sensitive inhibitor DFF45. Curr Biol *8*, 537-540.

Harlow, L.S., Kadziola, A., Jensen, K.F., and Larsen, S. (2004a). Crystal structure of the phosphorolytic exoribonuclease RNase PH from Bacillus subtilis and implications for its quaternary structure and tRNA binding. Protein Sci *13*, 668-677.

Harlow, L.S., Kadziola, A., Jensen, K.F., and Larsen, S. (2004b). Crystal structure of the phosphorolytic exoribonuclease RNase PH from *Bacillus subtilis* and implications for its quaternary structure and tRNA binding. Protein Sci *13*, 668-677.

Harrington, J.J., and Lieber, M.R. (1994). The characterization of a mammalian DNA structure-specific endonuclease. EMBO J *13*, 1235-1246.

Hedgecock, E.M., Sulston, J.E., and Thomson, J.N. (1983). Mutations affecting programmed cell deaths in the nematode Caenorhabditis elegans. Science *220*, 1277-1279.

Hilleren, P., McCarthy, T., Rosbash, M., Parker, R., and Jensen, T.H. (2001). Quality control of mRNA 3'-end processing is linked to the nuclear exosome. Nature *413*, 538-542.

Houseley, J., LaCava, J., and Tollervey, D. (2006). RNA-quality control by the exosome. Nat Rev Mol Cell Biol *7*, 529-539.

Houseley, J., and Tollervey, D. (2006). Yeast Trf5p is a nuclear poly(A) polymerase. EMBO Rep *7*, 205-211.

Hsiao, Y.Y., Nakagawa, A., Shi, Z., Mitani, S., Xue, D., and Yuan, H.S. (2009). Crystal structure of CRN-4: implications for domain function in apoptotic DNA degradation. Mol Cell Biol *29*, 448-457.

Hutvagner, G., McLachlan, J., Pasquinelli, A.E., Balint, E., Tuschl, T., and Zamore, P.D. (2001). A cellular function for the RNA-interference enzyme Dicer in the maturation of

the let-7 small temporal RNA. Science *293*, 834-838.
Inada, T., and Aiba, H. (2005). Translation of aberrant mRNAs lacking a termination codon or with a shortened 3'-UTR is repressed after initiation in yeast. EMBO J *24*, 1584-1595.
Irvine, R.A., Adachi, N., Shibata, D.K., Cassell, G.D., Yu, K., Karanjawala, Z.E., Hsieh, C.L., and Lieber, M.R. (2005). Generation and characterization of endonuclease G null mice. Mol Cell Biol *25*, 294-302.
Ishii, R., Nureki, O., and Yokoyama, S. (2003a). Crystal structure of the tRNA processing enzyme RNase PH from Aquifex aeolicus. J Biol Chem *278*, 32397-32404.
Ishii, R., Nureki, O., and Yokoyama, S. (2003b). Crystal structure of the tRNA processing enzyme RNase PH from *Aquifex aeolicus*. J Biol Chem *278*, 32397-32404.
Jensen, K.F., Andersen, J.T., and Poulsen, P. (1992). Overexpression and rapid purification of the orfE/rph gene product, RNase PH of Escherichia coli. J Biol Chem *267*, 17147-17152.
Kadaba, S., Krueger, A., Trice, T., Krecic, A.M., Hinnebusch, A.G., and Anderson, J. (2004). Nuclear surveillance and degradation of hypomodified initiator tRNAMet in S. cerevisiae. Genes Dev *18*, 1227-1240.
Kawane, K., Fukuyama, H., Yoshida, H., Nagase, H., Ohsawa, Y., Uchiyama, Y., Okada, K., Iida, T., and Nagata, S. (2003). Impaired thymic development in mouse embryos deficient in apoptotic DNA degradation. Nat Immunol *4*, 138-144.
Kawane, K., Ohtani, M., Miwa, K., Kizawa, T., Kanbara, Y., Yoshioka, Y., Yoshikawa, H., and Nagata, S. (2006). Chronic polyarthritis caused by mammalian DNA that escapes from degradation in macrophages. Nature *443*, 998-1002.
Kelly, K.O., Reuven, N.B., Li, Z., and Deutscher, M.P. (1992). RNase PH is essential for tRNA processing and viability in RNase-deficient Escherichia coli cells. J Biol Chem *267*, 16015-16018.
Kolb, H.J., Mittermuller, J., Clemm, C., Holler, E., Ledderose, G., Brehm, G., Heim, M., and Wilmanns, W. (1990). Donor leukocyte transfusions for treatment of recurrent chronic myelogenous leukemia in marrow transplant patients. Blood *76*, 2462-2465.
Kolb, H.J., Schattenberg, A., Goldman, J.M., Hertenstein, B., Jacobsen, N., Arcese, W., Ljungman, P., Ferrant, A., Verdonck, L., Niederwieser, D.*, et al.* (1995). Graft-versus-leukemia effect of donor lymphocyte transfusions in marrow grafted patients. Blood *86*, 2041-2050.
Koonin, E.V., Wolf, Y.I., and Aravind, L. (2001). Prediction of the archaeal exosome and its connections with the proteasome and the translation and transcription machineries by a comparative-genomic approach. Genome Res *11*, 240-252.
Krieser, R.J., MacLea, K.S., Longnecker, D.S., Fields, J.L., Fiering, S., and Eastman, A. (2002). Deoxyribonuclease IIalpha is required during the phagocytic phase of apoptosis

and its loss causes perinatal lethality. Cell Death Differ *9*, 956-962.

Krizman, D.B., Wagner, L., Lash, A., Strausberg, R.L., and Emmert-Buck, M.R. (1999). The Cancer Genome Anatomy Project: EST sequencing and the genetics of cancer progression. Neoplasia *1*, 101-106.

LaCava, J., Houseley, J., Saveanu, C., Petfalski, E., Thompson, E., Jacquier, A., and Tollervey, D. (2005). RNA degradation by the exosome is promoted by a nuclear polyadenylation complex. Cell *121*, 713-724.

Laskowski, R.A., MacArthur, M.W., Moss, D.S., and Thornton, J.M. (1993). PROCHECK: a program to check the stereochemical quality of protein structures. J Appl Cryst *26*, 283-291.

Lee, Y.S., Nakahara, K., Pham, J.W., Kim, K., He, Z., Sontheimer, E.J., and Carthew, R.W. (2004). Distinct roles for Drosophila Dicer-1 and Dicer-2 in the siRNA/miRNA silencing pathways. Cell *117*, 69-81.

Lejeune, F., Li, X., and Maquat, L.E. (2003). Nonsense-mediated mRNA decay in mammalian cells involves decapping, deadenylating, and exonucleolytic activities. Mol Cell *12*, 675-687.

Leszczyniecka, M., Kang, D.C., Sarkar, D., Su, Z.Z., Holmes, M., Valerie, K., and Fisher, P.B. (2002). Identification and cloning of human polynucleotide phosphorylase, hPNPase old-35, in the context of terminal differentiation and cellular senescence. Proc Natl Acad Sci U S A *99*, 16636-16641.

Li, L.Y., Luo, X., and Wang, X. (2001). Endonuclease G is an apoptotic DNase when released from mitochondria. Nature *412*, 95-99.

Li, Z., and Deutscher, M.P. (1994). The role of individual exoribonucleases in processing at the 3' end of Escherichia coli tRNA precursors. J Biol Chem *269*, 6064-6071.

Lieber, M.R. (1997). The FEN-1 family of structure-specific nucleases in eukaryotic DNA replication, recombination and repair. Bioessays *19*, 233-240.

Liu, J., Carmell, M.A., Rivas, F.V., Marsden, C.G., Thomson, J.M., Song, J.J., Hammond, S.M., Joshua-Tor, L., and Hannon, G.J. (2004). Argonaute2 is the catalytic engine of mammalian RNAi. Science *305*, 1437-1441.

Liu, Q., Greimann, J.C., and Lima, C.D. (2006). Reconstitution, activities, and structure of the eukaryotic RNA exosome. Cell *127*, 1223-1237.

Liu, Q., Rand, T.A., Kalidas, S., Du, F., Kim, H.E., Smith, D.P., and Wang, X. (2003a). R2D2, a bridge between the initiation and effector steps of the Drosophila RNAi pathway. Science *301*, 1921-1925.

Liu, Q.L., Kishi, H., Ohtsuka, K., and Muraguchi, A. (2003b). Heat shock protein 70 binds caspase-activated DNase and enhances its activity in TCR-stimulated T cells. Blood *102*, 1788-1796.

Liu, X., Li, P., Widlak, P., Zou, H., Luo, X., Garrard, W.T., and Wang, X. (1998). The 40-kDa subunit of DNA fragmentation factor induces DNA fragmentation and chromatin condensation during apoptosis. Proc Natl Acad Sci U S A *95*, 8461-8466.

Liu, X., Zou, H., Slaughter, C., and Wang, X. (1997). DFF, a heterodimeric protein that functions downstream of caspase-3 to trigger DNA fragmentation during apoptosis. Cell *89*, 175-184.

Liu, X., Zou, H., Widlak, P., Garrard, W., and Wang, X. (1999). Activation of the apoptotic endonuclease DFF40 (caspase-activated DNase or nuclease). Oligomerization and direct interaction with histone H1. J Biol Chem *274*, 13836-13840.

Long, F., Vagin, A.A., Young, P., and Murshudov, G.N. (2008). BALBES: a molecular-replacement pipeline. Acta Crystallogr D Biol Crystallogr *64*, 125-132.

Lorentzen, E., and Conti, E. (2005). Structural basis of 3' end RNA recognition and exoribonucleolytic cleavage by an exosome RNase PH core. Mol Cell *20*, 473-481.

Lorentzen, E., Dziembowski, A., Lindner, D., Seraphin, B., and Conti, E. (2007). RNA channelling by the archaeal exosome. EMBO Rep *8*, 470-476.

Lorentzen, E., Walter, P., Fribourg, S., Evguenieva-Hackenberg, E., Klug, G., and Conti, E. (2005). The archaeal exosome core is a hexameric ring structure with three catalytic subunits. Nat Struct Mol Biol *12*, 575-581.

Lykke-Andersen, S., Brodersen, D.E., and Jensen, T.H. (2009). Origins and activities of the eukaryotic exosome. J Cell Sci *122*, 1487-1494.

McIlroy, D., Sakahira, H., Talanian, R.V., and Nagata, S. (1999). Involvement of caspase 3-activated DNase in internucleosomal DNA cleavage induced by diverse apoptotic stimuli. Oncogene *18*, 4401-4408.

McIlroy, D., Tanaka, M., Sakahira, H., Fukuyama, H., Suzuki, M., Yamamura, K., Ohsawa, Y., Uchiyama, Y., and Nagata, S. (2000). An auxiliary mode of apoptotic DNA fragmentation provided by phagocytes. Genes Dev *14*, 549-558.

Mi, H., Kops, O., Zimmermann, E., Jaschke, A., and Tropschug, M. (1996). A nuclear RNA-binding cyclophilin in human T cells. FEBS Lett *398*, 201-205.

Mitchell, P., Petfalski, E., Shevchenko, A., Mann, M., and Tollervey, D. (1997). The exosome: a conserved eukaryotic RNA processing complex containing multiple 3'-->5' exoribonucleases. Cell *91*, 457-466.

Mitchell, P., and Tollervey, D. (2003). An NMD pathway in yeast involving accelerated deadenylation and exosome-mediated 3'-->5' degradation. Mol Cell *11*, 1405-1413.

Mukae, N., Yokoyama, H., Yokokura, T., Sakoyama, Y., and Nagata, S. (2002). Activation of the innate immunity in Drosophila by endogenous chromosomal DNA that escaped apoptotic degradation. Genes Dev *16*, 2662-2671.

Mukherjee, D., Gao, M., O'Connor, J.P., Raijmakers, R., Pruijn, G., Lutz, C.S., and Wilusz, J. (2002). The mammalian exosome mediates the efficient degradation of

mRNAs that contain AU-rich elements. EMBO J *21*, 165-174.

Nakagawa, A., Shi, Y., Kage-Nakadai, E., Mitani, S., and Xue, D. (2010). Caspase-dependent conversion of Dicer ribonuclease into a death-promoting deoxyribonuclease. Science *328*, 327-334.

Napirei, M., Karsunky, H., Zevnik, B., Stephan, H., Mannherz, H.G., and Moroy, T. (2000). Features of systemic lupus erythematosus in DNase I deficient mice. Nature Genet *25*, 177-181.

Navarro, M.V., Oliveira, C.C., Zanchin, N.I., and Guimaraes, B.G. (2008). Insights into the mechanism of progressive RNA degradation by the archaeal exosome. J Biol Chem *283*, 14120-14131.

Nurmohamed, S., Vaidialingam, B., Callaghan, A.J., and Luisi, B.F. (2009). Crystal structure of *Escherichia coli* polynucleotide phosphorylase core bound to RNase E, RNA and manganese: Implications for catalytic mechanism and RNA degradosome assembly. J Mol Biol *389*, 17-33.

Okabe, Y., Sano, T., and Nagata, S. (2009). Regulation of the innate immune response by threonine-phosphatase of Eyes absent. Nature *460*, 520-524.

Orban, T.I., and Izaurralde, E. (2005). Decay of mRNAs targeted by RISC requires XRN1, the Ski complex, and the exosome. RNA *11*, 459-469.

Otwinowski, Z., and Minor, W. (1997). Processing of X-ray diffraction data collected in oscillation mode. Methods Enzymol *276*, 307-326.

Parrish, J., Li, L., Klotz, K., Ledwich, D., Wang, X., and Xue, D. (2001). Mitochondrial endonuclease G is important for apoptosis in *C. elegans*. Nature *412*, 90-94.

Parrish, J.Z., and Xue, D. (2003a). Functional genomic analysis of apoptotic DNA degradation in *C. elegans*. Mol Cell *11*, 987-996.

Parrish, J.Z., and Xue, D. (2003b). Functional genomic analysis of apoptotic DNA degradation in *C. elegans*. Mol Cell *11*, 987-996.

Parrish, J.Z., and Xue, D. (2006). Cuts can kill: the roles of apoptotic nucleases in cell death and animal development. Chromosoma *115*, 89-97.

Parrish, J.Z., Yang, C., Shen, B., and Xue, D. (2003). CRN-1, a *Caenorhabditis elegans* FEN-1 homologue, cooperates with CPS-6/EndoG to promote apoptotic DNA degradation. EMBO J *22*, 3451-3460.

Pham, J.W., Pellino, J.L., Lee, Y.S., Carthew, R.W., and Sontheimer, E.J. (2004). A Dicer-2-dependent 80s complex cleaves targeted mRNAs during RNAi in Drosophila. Cell *117*, 83-94.

Piwowarski, J., Grzechnik, P., Dziembowski, A., Dmochowska, A., Minczuk, M., and Stepien, P.P. (2003). Human polynucleotide phosphorylase, hPNPase, is localized in mitochondria. J Mol Biol *329*, 853-857.

Potterton, E., Briggs, P., Turkenburg, M., and Dodson, E. (2003). A graphical user

interface to the CCP4 program suite. Acta Crystallogr D Biol Crystallogr *59*, 1131-1137.

Raijmakers, R., Schilders, G., and Pruijn, G.J. (2004). The exosome, a molecular machine for controlled RNA degradation in both nucleus and cytoplasm. Eur J Cell Biol *83*, 175-183.

Reichlin, M., Maddison, P.J., Targoff, I., Bunch, T., Arnett, F., Sharp, G., Treadwell, E., and Tan, E.M. (1984). Antibodies to a nuclear/nucleolar antigen in patients with polymyositis overlap syndromes. J Clin Immunol *4*, 40-44.

Rivas, F.V., Tolia, N.H., Song, J.J., Aragon, J.P., Liu, J., Hannon, G.J., and Joshua-Tor, L. (2005). Purified Argonaute2 and an siRNA form recombinant human RISC. Nat Struct Mol Biol *12*, 340-349.

Sakahira, H., Enari, M., and Nagata, S. (1998). Cleavage of CAD inhibitor in CAD activation and DNA degradation during apoptosis. Nature *391*, 96-99.

Samejima, K., and Earnshaw, W.C. (2005). Trashing the genome: the role of nucleases during apoptosis. Nat Rev Mol Cell Biol *6*, 677-688.

Schaeffer, D., Tsanova, B., Barbas, A., Reis, F.P., Dastidar, E.G., Sanchez-Rotunno, M., Arraiano, C.M., and van Hoof, A. (2009). The exosome contains domains with specific endoribonuclease, exoribonuclease and cytoplasmic mRNA decay activities. Nat Struct Mol Biol *16*, 56-62.

Schmid, M., and Jensen, T.H. (2008). The exosome: a multipurpose RNA-decay machine. Trends Biochem Sci *33*, 501-510.

Schuck, P. (2000). Size-distribution analysis of macromolecules by sedimentation velocity ultracentrifugation and lamm equation modeling. Biophys J *78*, 1606-1619.

Shi, Z., Yang, W.Z., Lin-Chao, S., Chak, K.F., and Yuan, H.S. (2008). Crystal structure of *Escherichia coli* PNPase: central channel residues are involved in processive RNA degradation. RNA *14*, 2361-2371.

Stickney, L.M., Hankins, J.S., Miao, X., and Mackie, G.A. (2005). Function of the conserved S1 and KH domains in polynucleotide phosphorylase. J Bacteriol *187*, 7214-7221.

Suzuki, N., Noguchi, E., Nakashima, N., Oki, M., Ohba, T., Tartakoff, A., Ohishi, M., and Nishimoto, T. (2001). The Saccharomyces cerevisiae small GTPase, Gsp1p/Ran, is involved in 3' processing of 7S-to-5.8S rRNA and in degradation of the excised 5'-A0 fragment of 35S pre-rRNA, both of which are carried out by the exosome. Genetics *158*, 613-625.

Symmons, M.F., Jones, G.H., and Luisi, B.F. (2000). A duplicated fold is the structural basis for polynucleotide phosphorylase catalytic activity, processivity, and regulation. Structure *8*, 1215-1226.

Symmons, M.F., Williams, M.G., Luisi, B.F., Jones, G.H., and Carpousis, A.J. (2002).

Running rings around RNA: a superfamily of phosphate-dependent RNases. Trends Biochem Sci *27*, 11-18.

Takahashi, S., Araki, Y., Sakuno, T., and Katada, T. (2003). Interaction between Ski7p and Upf1p is required for nonsense-mediated 3'-to-5' mRNA decay in yeast. EMBO J *22*, 3951-3959.

Thiebaut, M., Kisseleva-Romanova, E., Rougemaille, M., Boulay, J., and Libri, D. (2006). Transcription termination and nuclear degradation of cryptic unstable transcripts: a role for the nrd1-nab3 pathway in genome surveillance. Mol Cell *23*, 853-864.

Thomas, D.A., Du, C., Xu, M., Wang, X., and Ley, T.J. (2000). DFF45/ICAD can be directly processed by granzyme B during the induction of apoptosis. Immunity *12*, 621-632.

Toh, S.Y., Wang, X., and Li, P. (1998). Identification of the nuclear factor HMG2 as an activator for DFF nuclease activity. Biochem Biophys Res Commun *250*, 598-601.

Torchet, C., Bousquet-Antonelli, C., Milligan, L., Thompson, E., Kufel, J., and Tollervey, D. (2002). Processing of 3'-extended read-through transcripts by the exosome can generate functional mRNAs. Mol Cell *9*, 1285-1296.

Tran, H., Schilling, M., Wirbelauer, C., Hess, D., and Nagamine, Y. (2004). Facilitation of mRNA deadenylation and decay by the exosome-bound, DExH protein RHAU. Mol Cell *13*, 101-111.

Treadwell, E.L., Alspaugh, M.A., Wolfe, J.F., and Sharp, G.C. (1984). Clinical relevance of PM-1 antibody and physiochemical characterization of PM-1 antigen. J Rheumatol *11*, 658-662.

U.Z. Littauer and M. Grunberg-Manago (1999). Polynucleotide Phosphorylase, in: T.E. Creighton (Ed.). The Encyclopedia of Molecular Biology, John Willy and Sons Inc, New York, 1911-1918.

Vahsen, N., Cande, C., Briere, J.J., Benit, P., Joza, N., Larochette, N., Mastroberardino, P.G., Pequignot, M.O., Casares, N., Lazar, V., *et al.* (2004). AIF deficiency compromises oxidative phosphorylation. EMBO J *23*, 4679-4689.

van Dijk, E.L., Schilders, G., and Pruijn, G.J. (2007). Human cell growth requires a functional cytoplasmic exosome, which is involved in various mRNA decay pathways. RNA *13*, 1027-1035.

van Hoof, A., Frischmeyer, P.A., Dietz, H.C., and Parker, R. (2002). Exosome-mediated recognition and degradation of mRNAs lacking a termination codon. Science *295*, 2262-2264.

van Hoof, A., Lennertz, P., and Parker, R. (2000a). Yeast exosome mutants accumulate 3'-extended polyadenylated forms of U4 small nuclear RNA and small nucleolar RNAs. Mol Cell Biol *20*, 441-452.

van Hoof, A., Staples, R.R., Baker, R.E., and Parker, R. (2000b). Function of the ski4p

(Csl4p) and Ski7p proteins in 3'-to-5' degradation of mRNA. Mol Cell Biol *20*, 8230-8243.

Vanacova, S., Wolf, J., Martin, G., Blank, D., Dettwiler, S., Friedlein, A., Langen, H., Keith, G., and Keller, W. (2005). A new yeast poly(A) polymerase complex involved in RNA quality control. PLoS Biol *3*, e189.

Vasiljeva, L., and Buratowski, S. (2006). Nrd1 interacts with the nuclear exosome for 3' processing of RNA polymerase II transcripts. Mol Cell *21*, 239-248.

Wang, L., Lewis, M.S., and Johnson, A.W. (2005). Domain interactions within the Ski2/3/8 complex and between the Ski complex and Ski7p. RNA *11*, 1291-1302.

Wang, X., Yang, C., Chai, J., Shi, Y., and Xue, D. (2002). Mechanisms of AIF-mediated apoptotic DNA degradation in Caenorhabditis elegans. Science *298*, 1587-1592.

Widlak, P., Li, P., Wang, X., and Garrard, W.T. (2000). Cleavage preferences of the apoptotic endonuclease DFF40 (caspase-activated DNase or nuclease) on naked DNA and chromatin substrates. J Biol Chem *275*, 8226-8232.

Wolf, B.B., Schuler, M., Echeverri, F., and Green, D.R. (1999). Caspase-3 is the primary activator of apoptotic DNA fragmentation via DNA fragmentation factor-45/inhibitor of caspase-activated DNase inactivation. J Biol Chem *274*, 30651-30656.

Wu, C.J., Yang, X.F., McLaughlin, S., Neuberg, D., Canning, C., Stein, B., Alyea, E.P., Soiffer, R.J., Dranoff, G., and Ritz, J. (2000a). Detection of a potent humoral response associated with immune-induced remission of chronic myelogenous leukemia. J Clin Investig *106*, 705-714.

Wu, Y.C., Stanfield, G.M., and Horvitz, H.R. (2000b). NUC-1, a *Caenorhabditis elegans* DNase II homolog, functions in an intermediate step of DNA degradation during apoptosis. Genes & Develop *14*, 536-548.

Wyers, F., Rougemaille, M., Badis, G., Rousselle, J.C., Dufour, M.E., Boulay, J., Regnault, B., Devaux, F., Namane, A., Seraphin, B.*, et al.* (2005). Cryptic pol II transcripts are degraded by a nuclear quality control pathway involving a new poly(A) polymerase. Cell *121*, 725-737.

Wyllie, A.H. (1980). Glucocorticoid-induced thymocyte apoptosis is associated with endogenous endonuclease activation. Nature *284*, 555-556.

Xie, L.-H., Sin, F.W.-Y., Cheng, S.C.-S., Cheung, Y.-K., Chan, K.-T., Xie, Y., and Xie, Y. (2008). Activation of cytotoxic T lymphocytes against CML28-bearing tumors by dendritic cells transduced with a recombinant adeno-associated virus encoding the CML28 gene. Cancer Immunol Immunother *57*, 1029-1038.

Yang, X.-F., Wu, C.J., Chen, L., Alyea, E.P., Canning, C., Kantoff, P., Soiffer, R.J., Dranoff, G., and Ritz, J. (2002). CML28 is a broadly immunogenic antigen, which is

overexpressed in tumor cells. Cancer Res *62*, 5517-5522.
Yang, X.C., Purdy, M., Marzluff, W.F., and Dominski, Z. (2006). Characterization of 3'hExo, a 3' exonuclease specifically interacting with the 3' end of histone mRNA. J Biol Chem *281*, 30447-30454.
Yasutomo, K., Horiuchi, K., Kagami, T., Tsukamoto, H., Hashimura, C., Urushihara, M., and Kuroda, Y. (2001). Mutation of DNASE1 in people with systemic lupus erythematosus. Nature Genet *28*, 313-314.
Yeates, T.O. (1997). Detecting and overcoming crystal twinning. Methods Enzymol *276*, 344-358.
Yokoyama, H., Mukae, N., Sakahira, H., Okawa, K., Iwamatsu, A., and Nagata, S. (2000). A novel activation mechanism of caspase-activated DNase from Drosophila melanogaster. J Biol Chem *275*, 12978-12986.
Zanchin, N.I., and Goldfarb, D.S. (1999). The exosome subunit Rrp43p is required for the efficient maturation of 5.8S, 18S and 25S rRNA. Nucleic Acids Res *27*, 1283-1288.
Zhang, H., Kolb, F.A., Brondani, V., Billy, E., and Filipowicz, W. (2002). Human Dicer preferentially cleaves dsRNAs at their termini without a requirement for ATP. EMBO J *21*, 5875-5885.
Zhang, H., Kolb, F.A., Jaskiewicz, L., Westhof, E., and Filipowicz, W. (2004). Single processing center models for human Dicer and bacterial RNase III. Cell *118*, 57-68.
Zhang, J., Liu, X., Scherer, D.C., van Kaer, L., Wang, X., and Xu, M. (1998). Resistance to DNA fragmentation and chromatin condensation in mice lacking the DNA fragmentation factor 45. Proc Natl Acad Sci U S A *95*, 12480-12485.
Zhou, H., Zhang, D., Wang, Y., Dai, M., Zhang, L., Liu, W., Liu, D., Tan, H., and Huang, Z. (2006). Induction of CML28-specific cytotoxic T cell responses using co-transfected dendritic cells with CML28 DNA vaccine and SOCS1 small interfering RNA expression vector. Biochem Biophys Res Commun *347*, 200-207.